



1

2 **Polar semi-volatile organic compounds in biomass burning emissions and their**  
3 **chemical transformations during aging in an oxidation flow reactor**

4 Deep Sengupta,<sup>1</sup> Vera Samburova,<sup>1</sup> Chiranjivi Bhattarai,<sup>1</sup> Adam C. Watts,<sup>1</sup> Hans Moosmüller,<sup>1</sup>  
5 Andrey Y. Khlystov<sup>1</sup>

6 <sup>1</sup>Desert Research Institute, 2215 Raggio Parkway, Reno, NV 89512, USA

7

8

9 *Correspondence to:* vera.samburova@dri.edu

10 **Abstract**

11 Semi-volatile organic compounds (SVOCs) emitted from open biomass-burning (BB) can  
12 contribute to chemical and physical properties of atmospheric aerosols and also may cause adverse  
13 health effects. The polar fraction of SVOCs constitutes a significant part of BB organic aerosols,  
14 and thus it is important to characterize the chemical composition and reactivity of this fraction. In  
15 this study, globally and regionally important representative fuels (Alaskan peat, Moscow peat,  
16 Pskov peat, Eucalyptus, Malaysian peat, and Malaysian agricultural peat) were burned under  
17 controlled conditions using the combustion chamber facility at the Desert Research Institute (DRI).  
18 Gas- and particulate-phase biomass-burning emissions were aged in an oxidation flow reactor  
19 (OFR) to mimic 5–7 days of atmospheric aging. Fresh and OFR-aged biomass-burning aerosols  
20 were collected on Teflon impregnated glass fiber filters (TIGF) in tandem with XAD resin media  
21 for organic compound (OC) speciation. The polar fraction extracted with dichloromethane and  
22 acetone was analyzed with gas chromatography mass spectrometry (GC-MS) for 84 polar organic  
23 compounds—including mono and dicarboxylic acids, methoxylated phenols, aromatic acids,  
24 anhydrosugars, resin acids, and sterols. For all these compounds, fuel-based emission factors (EFs)  
25 were calculated for fresh and OFR-aged samples. The carbon mass of the quantified polar  
26 compounds was found to constitute 5% to 7% of the total OC mass. High abundance of  
27 methoxyphenols (239 mg kg<sup>-1</sup> for Pskov peat; 22.6% of total GC-MS characterized mass) and resin  
28 acids (118 mg kg<sup>-1</sup> for Pskov peat; 14.5 % of total GC-MS characterized mass) was found in peat  
29 burning emissions (smoldering combustion). Concentration of some organic compounds (e.g.,  
30 tetracosanoic acid) with molecular weight (MW) above 350 g mol<sup>-1</sup> decreased after the OFR aging,  
31 while abundances of low MW compounds (e.g., hexanoic acid) increased. This indicated a  
32 significant extent of fragmentation reactions in the OFR. Methoxyphenols decreased after OFR



33 aging, while a significant increase (3.7 to 8.6 times) in abundance of dicarboxylic acids emission  
34 factors (EFs), especially maleic acid (10 to 60 times), was observed. EFs for fresh and ratios from  
35 fresh-to-aged BB samples reported in this study can be used to perform source apportionment and  
36 predict processes occurring during atmospheric transport.

37

38

39 **Keywords.** Biomass burning, organic aerosols, semi-volatile organic compounds (SVOCs), gas  
40 chromatography, mass spectrometry, polar organic compounds, oxidation flow reactor

41



## 42 **1 Introduction**

43 Biomass burning (BB), including both wildfires and prescribed burns, is a major source of  
44 carbonaceous aerosols in the atmosphere (Penner et al., 1991) and can contribute up to 75% of  
45 total atmospheric aerosol mass loading (Andreae et al., 2001; Park et al., 2007). These  
46 carbonaceous aerosols have significant impact on both regional and global radiative forcing  
47 (Ramanathan and Carmichael, 2008). BB emissions also can cause adverse health effects (Arbex  
48 et al., 2007; Regalado et al., 2006) because of the mutagenic property of particle-bound organic  
49 compounds (Yang et al., 2010). Therefore, comprehensive, molecular-level characterization of BB  
50 emissions is essential for understanding health effects. Such molecular characterization of BB  
51 carbonaceous aerosols in the atmosphere, however, is challenging as these aerosols are composed  
52 of tens of thousands of compounds (Goldstein and Galbally, 2007).

53

54 Current atmospheric chemistry models use a limited number of organic species because of the  
55 complexity of atmospheric aerosol chemical composition and the lack of aerosol chemical  
56 speciation data. Approximately 80% of BB organic mass emissions, especially aged emissions, are  
57 not identified in such models (Bertrand et al., 2018; Jen et al., 2019), limiting the capabilities of  
58 atmospheric organic aerosol modeling. Thus, improvement is needed in molecular-level speciation  
59 of both fresh and aged BB emissions for more accurate model estimations.

60

61 Simulation of natural fires in a laboratory environment using a BB chamber is one way to  
62 characterize the chemical composition of BB emissions (Yokelson et al., 2003). A number of  
63 studies characterizing the molecular composition of combustion emissions from fuels that  
64 represent different geographical regions have been completed: temperate conifers (Oros and  
65 Simoneit, 2001a), deciduous trees (Oros and Simoneit, 2001b), grasses (Oros et al., 2006), and  
66 peats (Samburova et al., 2016; Iinuma et al., 2007). Akagi et al. (2011) compiled fuel-based  
67 emission factors (EFs) from different fuels from throughout the world, including the peatlands of  
68 south Asia, and found that burning condition (flaming/smoldering) can influence the EFs of  
69 individual compounds. These data have been used for modeling work in predicting ozone-forming  
70 potential and other air quality impacts (Alvarado et al., 2015). Most of these source apportionment  
71 studies, however, were focused on characterization of fresh emissions and emissions of either  
72 particle-phase or gas-phase compounds.



73

74 Significant changes in organic aerosol composition during atmospheric transport have been  
75 reported (Liu et al., 2017; Decker et al., 2019). These changes can impact local and regional air  
76 quality. Also, the role of Siberian peat burning in haze formation in the Korean peninsula (Jung et  
77 al., 2016) demonstrates the global impact of BB emissions and their atmospheric transport on  
78 regional air quality. Some laboratory studies found an increase in organic aerosol (OA) mass after  
79 photochemical aging (Ortega et al., 2013; Grieshop et al., 2009) while others observed a modest  
80 decrease (Bhattacharai et al., 2018). There is still limited data on evolution of chemical composition  
81 of primary organic aerosols (POAs) during atmospheric aging. Some laboratory experiments  
82 demonstrated degradation of levoglucosan (Hennigan et al., 2010; Kessler et al., 2010) and  
83 oxidation of methoxyphenols in the gas phase (Yee et al., 2013) and aqueous phase (Net et al.,  
84 2011). These studies have more mechanistic implications than quantifying gross change after  
85 atmospheric oxidation. Recently, Fortenberry et al. (2018) characterized the chemical fingerprints  
86 of aged biomass-burning aerosols (leaf and hardwood of white oak) by performing oxidation in a  
87 potential aerosol mass oxidation flow reactor (PAM-OFR) and chemical analysis with a thermal  
88 desorption aerosol gas chromatograph aerosol mass spectrometer (TAG-AMS). Bertrand et al.  
89 (2018) analyzed 71 organic compounds in BB emissions, sampled from a smog chamber, with  
90 high resolution time of flight mass spectrometry (HR-ToF-AMS). There is still a lack of  
91 understanding, however, regarding (1) major organic compounds emitted from BB, (2) their roles  
92 in atmospheric photochemical reactions, and (3) what compounds are responsible for light  
93 absorption of fresh and aged BB emissions.

94

95 In this study, emissions from laboratory combustion of six globally important fuels (Alaskan peat,  
96 Moscow peat, Pskov peat, Eucalyptus, Malaysian peat, and Malaysian agricultural peat) were  
97 quantitatively analyzed for more than 250 individual organic species, and analyses of 84 polar  
98 organic species is presented in this paper. BB emissions generated in a combustion chamber were  
99 run through the OFR, mimicking approximately 5 to 7 days of atmospheric oxidation (Bhattacharai et  
100 al., 2018b), and the OFR output was analyzed to characterize aged BB emissions. BB emissions  
101 were collected on filter and XAD media to identify distribution of organic species between the gas  
102 and particle phases. For the polar fraction of collected organic compounds, we quantitatively  
103 analyzed a total of 84 compounds (methoxyphenol derivatives, dicarboxylic acids,



104 monocarboxylic acids, aromatic acids, resin acids, and anhydrosugars). In the analyzed  
105 anhydrosugars, we paid special attention to levoglucosan, a derivative from cellulose (Simoneit et  
106 al., 1999), since levoglucosan has been widely used as a molecular tracer of BB emissions  
107 (Bonvalot et al., 2016; Maenhaut et al., 2016). Methoxyphenols also have been used in source  
108 apportionment studies (Schauer et al., 2001a; Schmidl et al., 2008b, 2008a). These source  
109 apportionment studies, however, haven't combined such a wide range of different groups in a  
110 single investigation. Here we provide a detailed targeted chemical analysis of both gas- and  
111 particle-phase BB emissions from the combustion of individual biomass fuels from diverse  
112 geographical locations for both fresh and aged emissions. EFs of gas- and particulate-phase  
113 individual polar organic species are presented for six groups of compounds (methoxyphenols,  
114 dicarboxylic acids, monocarboxylic acids, aromatic acids, anhydrosugars, and resin acids) and are  
115 discussed in separate sections for fresh and OFR-aged BB samples. The fresh-to-aged ratio and  
116 top contributing organic species also are discussed. The comparison between fresh and OFR-aged  
117 BB emissions helps to understand the chemical evolution of BB plumes in the atmosphere and the  
118 obtained data can be used in future source apportionment and atmospheric modeling studies.  
119

## 120 **2. Experiments**

### 121 **2.1 Fuel Description**

122 We selected six globally and regionally important BB fuels: Alaskan peat, Moscow peat, Pskov  
123 peat, Eucalyptus, Malaysian peat, and Malaysian agricultural peat. Five of these were peat fuels  
124 selected from different geographical locations, representing smoldering combustion and one  
125 (Eucalyptus) representing flaming combustion.

126 Peatland ecosystems, generally wetland or mesic ecosystems underlain by soils composed  
127 primarily of partially-decomposed biomass, contain mostly organic carbon and more than 20%  
128 mineral content, represent a vast terrestrial carbon pool, and are potentially vast sources of carbon  
129 flux to the atmosphere during wildfires that consume peat (Harden et al., 2000). Peatlands in high-  
130 latitude temperate and boreal regions are particularly vulnerable to increased fire-related carbon  
131 emissions resulting from climatic warming and increases in fire season length, while peatlands in  
132 low-latitude and tropical regions are threatened by factors such as deforestation for agriculture,



133 urbanization, and drainage (Turetsky et al., 2015). We collected Alaskan peat samples from the  
134 upper 10 cm of soils within black spruce (*Picea mariana*) near crown forest (Chakrabarty et al.,  
135 2016). High-latitude and Eurasia samples here are from *Sphagnum*- and cotton grass- (*Eriophorum*  
136 spp.) dominated communities, collected from the Moscow (Odintsovo and Shatura districts) and  
137 Pskov regions of Russia. These regions are representative of oligotrophic peat bogs found widely  
138 across Siberia as well. Tropical peat in this study includes samples from two areas in Malaysian  
139 Borneo. One set of samples is from a *Dipterocarp*-dominated lowland forest with largely intact  
140 native land cover, while the second set is from a cleared agricultural area in the Kota Snamarahan  
141 region.

142

143 We selected Eucalyptus because of its prevalence across Australia and its important contribution  
144 to Australian wildland fires. In addition, economic losses and risk to life and property from fires  
145 in eucalypt forests are magnified by their proximity to both fire-prone ecosystems and large urban  
146 areas; often eucalypt-dominated stands form boundaries between these two land-use types. There  
147 are nearly 900 species of the genera *Eucalyptus*, *Corymba*, and *Angophora*, which collectively  
148 comprise woody plants known as eucalypts. Native to Australia, eucalypt-dominated forests cover  
149 nearly 92 million ha (Hills, W.E.; Brown, 1978). In addition, the fast and hardy growth  
150 characteristics of eucalypts have made them popular in warm ecoregions of Europe as well as  
151 North and South America, where they readily escape cultivation and become established, dominant  
152 community types near urban areas where they were originally introduced. Because of their high  
153 oil content, rapid and dense growth, and vegetative structure, eucalypts are highly flammable and  
154 contribute to high fire risk in areas where they occur (Goodrick and Stanturf, 2012).

155

## 156 **2.2 Reagents and Materials**

157 We obtained high-performance liquid chromatography (HPLC) grade methanol and hexane from  
158 Fisher Scientific (Fair Lawn, NJ, USA) and used the following filters for sampling and further  
159 chemical analyzes: pre-fired (900 °C for 4 h) 47 mm diameter quartz-fiber filter (2500 Pallflex  
160 QAT-UP, Pall Life Sciences, Ann Arbor, MI, USA) for thermo-optical Elemental Carbon/Organic  
161 carbon (EC/OC) analysis, Teflon® filters (2500 Pallflex QAT-UP, Pall Life Science, Ann Arbor,  
162 MI, USA) for gravimetric particulate matter (PM) mass analysis, and Teflon-impregnated glass

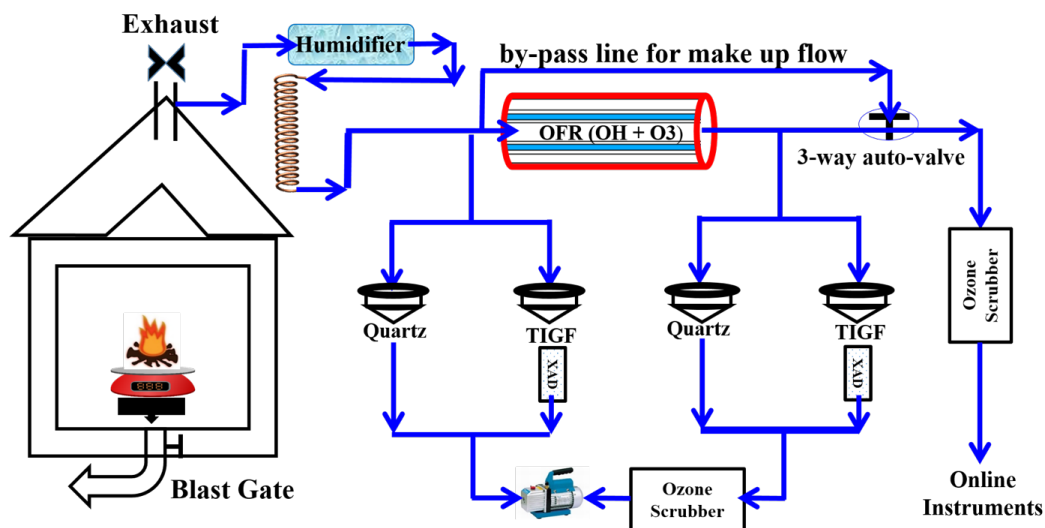


163 fiber (TIGF) 47 mm diameter filters (Fiber FilmT60A20, Pall Life Sciences, Ann Arbor, MI, USA)  
164 for organic analysis. We purchased the following deuterated internal standards from Cambridge  
165 isotope laboratories (Tewksbury, MA, USA) and CDN isotopes (Pointe-Claire, Quebec, Canada):  
166 hexanoic-d11 acid, benzoic-d5 acid, succinic-d4 acid, decanoic-d19 acid, adipic-d10 acid, suberic-  
167 d12 acid, levoglucosan-13C6, homovanillic-2,2-d2 acid, myristic-d27 acid, heptadecanoic33  
168 acid, oleic-9,10-d2 acid, tetradecanedioic-d24 acid, and cholesterol-2,2,3,4,4,6-d6.

169

170

### 171 2.3 Biomass Burning (BB) Experiments



172

173 **Figure 1.** Desert Research Institute (DRI) biomass burning (BB) facility with oxidative flow  
174 reactor (OFR) and flow setup.

175

176 BB experiments were conducted using DRI's BB facility for combustion of the selected fuels  
177 under controlled conditions. A close replicate of this facility was described previously (Tian et al.,  
178 2015), and a detailed description of the experimental setup was presented elsewhere (Bhattarai et  
179 al., 2018; Sengupta et al., 2018).

180

181 We mixed laboratory-generated BB emissions with humidified zero air (Airgas Inc., Sparks, NV,  
182 USA) using 4 m long spiral copper tubing (12.7 mm OD). Before it was mixed with the BB



183 emissions, the zero air was humidified by bubbling through Nano-pure water in a glass 500 mL  
184 volume impinger. The flow rate was controlled with a mass flow controller (810C-CE-RFQ-1821,  
185 Sierra Instruments, Monterey, CA, USA). An oxidation flow reactor (OFR) (Aerodyne Research  
186 Inc., Billerica, MA, USA) was used to mimic approximately seven days of equivalent atmospheric  
187 aging (Bhattacharai et al., 2018a). The OFR consisted of an alodine-coated aluminum cylinder (46 cm  
188 length and 22 cm diameter) with an internal volume of 13.3 L. Two sets of lamps emitted UV  
189 radiation at wavelengths of 185 and 254 nm (Atlantic Ultraviolet Corporation, Hauppauge, NY,  
190 USA) in the OFR to produce ozone and OH radicals (Li et al., 2015). UV irradiance in the OFR  
191 was quantified using a photodiode detector with a wavelength range of 225 to 287 nm  
192 (TOCON\_C6; Sglux GmbH, Berlin, Germany). Ultra-high-purity nitrogen (Airgas Inc., Reno,  
193 NV, USA) was used to purge the UV lamp compartments to prevent the lamps from overheating.  
194 A probe that monitored relative humidity and temperature inside the OFR (from Aerodyne Inc.,  
195 MA, USA) was mounted toward the outlet side of the OFR. A detailed characterization of the  
196 OFR—such as particle loss, OH production rate, and time scales of various processes—can be  
197 found in Bhattacharai et al. (2018).

198

199 The duration of smoldering combustion experiments ranged from 69 to 255 min, whereas the  
200 average duration of flaming combustion experiments was 50 min. During all experiments, both  
201 fresh (directly from the chamber) and aged (oxidized in the OFR) emissions were continuously  
202 collected on a TIGF filter (for particle phase) followed by an XAD cartridge (for gas phase) for  
203 detailed chemical speciation. We used several online instruments to characterize gas- and particle-  
204 phase pollutants (see Fig. 1). Simultaneous collection of samples for thermal optical carbon  
205 analysis on quartz fiber filters (Pall-Gelman, 47 mm diameter, pre-heated) was conducted, but only  
206 for Eucalyptus and Malaysian peat. The online instruments alternated every 10 min between  
207 sampling fresh and aged emissions using a computer-controlled valve system.

208

209 We employed a bypass flow to keep the flow from the BB chamber and through the OFR constant  
210 when online instruments switched between sampling fresh and aged emissions. To protect online  
211 instruments from high ozone concentrations produced in the OFR, ozone scrubbers were installed  
212 in front of the instruments' inlets. The ozone scrubbers were loaded with charcoal followed by  
213 Carulite 200 catalyst (Carus Corp., Peru, IL, USA). There were no ozone scrubbers before the





214 filter-XAD set up, which could cause further oxidation of organic compounds on filter surfaces  
215 during sampling. The reaction rates between organics and ozone, however, are orders of magnitude  
216 lower than OH oxidation reactions (Finlayson-Pitts and Pitts Jr, 1999). Therefore, we assumed that  
217 reactions with OH radicals were primarily responsible for changes in organic compounds  
218 associated with fresh gas and particulate emissions.

219

#### 220 **2.4. Organic and Elemental Carbon (OC/EC) Analysis**

221 Emissions from the combustion of two fuels (Eucalyptus and Malaysian peat) were sampled with  
222 quartz-fiber filters, collected simultaneously with TIGF filters, for both fresh and aged BB aerosols  
223 (Supplementary Material, Fig. S1). Punches (area = 1.5 cm<sup>2</sup>) from these quartz filters were  
224 analyzed with a thermal-optical carbon analyzer (Atmoslytic Inc., Calabasas, CA, USA) following  
225 the IMPROVE protocol (Chow et al., 1993, 2004) for total organic carbon (OC<sub>Total</sub>) and elemental  
226 carbon (EC) mass.

227

#### 228 **2.5 Analytical Methodology for GC-MS**

229 We extracted filter and XAD samples for GC/MS analysis (SI Table S1) yielding concentrations  
230 of 84 polar organic compounds. In addition, levoglucosan concentrations were determined using  
231 ion chromatography coupled with a pulsed amperometric detector (IC-PAD). Prior to the  
232 extraction, sampled TIGF filters and XAD-resin cartridges were spiked with deuterated internal  
233 standards (see “Reagents and Materials” section). The TIGF filters and XAD cartridges were  
234 extracted separately with an accelerated solvent extractor (Dionex ASE-300, Sunnyvale, CA,  
235 USA) at the following conditions: 80° C temperature, 250 mL extraction volume, and subsequent  
236 extraction with dichloromethane and acetone. The XAD and filters were treated separately to  
237 evaluate the speciation of gas- and particle-phase semi-volatile polar compounds. The extracts  
238 were concentrated with a rotary evaporator (Buchi-R124, Switzerland), filtered using 0.2 μm pore  
239 size syringe filters (Thermo Scientific, Redwood, TN, USA), and pre-concentrated with nitrogen  
240 to a volume of 4 mL. Then we split the extracts into two fractions. One fraction was transferred to  
241 2.0 mL volume deactivated glass maximum recovery vials (Waters Corporation, Milford, MA,  
242 USA), pre-concentrated to 50 μL volume under ultra-high-purity nitrogen (Airgas, Reno, NV,  
243 USA), and derivatized with N,O-bis-(trimethylsilyl) trifluoroacetamide (BSTFA with 1% of



244 trimethylchlorosilane; Thermo-Scientific, Bellefonte, PA, USA) and pyridine as described  
245 elsewhere (Rinehart et al., 2006). Derivatized samples were analyzed by electron impact ionization  
246 using a Varian CP-3400 gas chromatograph with a CP-8400 auto-sampler and interfaced to a  
247 Varian 4000 ion trap mass spectrometer (Varian Inc. Palo Alto, CA, USA). The second fraction of  
248 non-derivatized extracts was kept for further analysis of non-polar organic species (e.g., alkanes  
249 and PAHs), and those results will be presented in future publications.

250

## 251 **2.6. Levoglucosan Analysis**

252 Portions of quartz filters collected for OC/EC analysis also were used for quantitative analysis of  
253 levoglucosan concentration with IC-PAD. Prior to the analysis, quartz filters were extracted with  
254 15 ml of deionized water (18.2 MΩ), sonicated for one hour, and refrigerated overnight. The  
255 column temperature for IC was 25° C. Analytes along with a mixture of two eluents (48%  
256 hydroxide solution and 52% deionized water) were passed through the IC column with a 0.4 ml  
257 min<sup>-1</sup> eluent flow rate and detected using an electrochemical detector. See Chow and Watson  
258 (2017) for details.

259

260

261

## 262 **3. Results and Discussion**

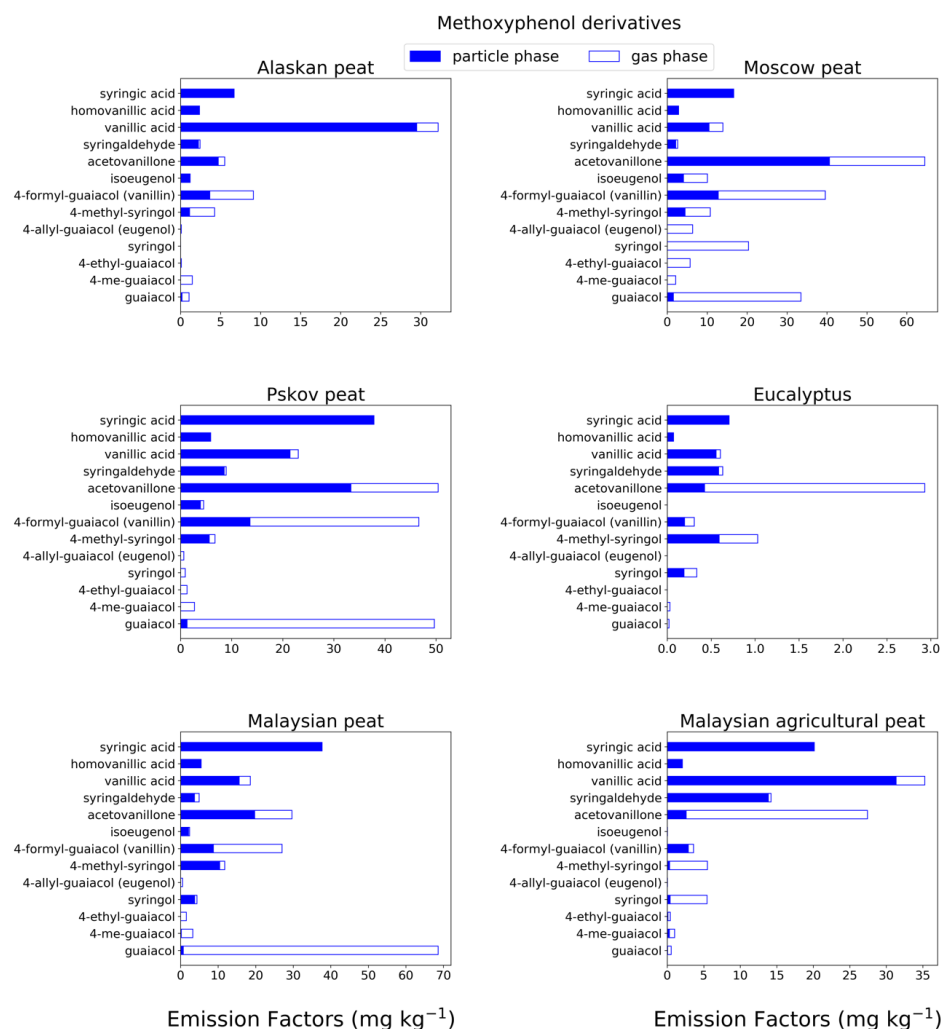
263

### 264 **3.1. Gas- and Particulate-Phase Emission Factors**

265 Organic compounds (84 in total) in fresh emissions identified and quantified in this study were  
266 assigned to six major groups (Table S1): methoxyphenol derivatives, dicarboxylic acids, mono-  
267 carboxylic acids, aromatic acids, resin acids, and levoglucosan. First, we report individual  
268 emission factors (EF) belonging to a particular group calculated by summation of gas- and particle-  
269 phase EFs of individual compounds. Relative abundance of these compounds are reported next  
270 followed by a comparison of the contributions of each group (EF<sub>group</sub>) among fuels and a  
271 comparison with previously reported results.

#### 272 **3.1.1 Methoxyphenol Derivatives**

273



274

275 Figure 2a. EFs for methoxyphenols in both particulate phase (solid bars, filter samples) and  
276 gas phase (open bars, XAD samples) from fresh biomass burning emissions for six different fuel types.  
277 We did not burn fuels in replicates, and standard deviations (SD) were calculated based on replicate  
278 analysis of emissions from similar fuels (with identical experimental conditions) during our  
279 previous combustion campaigns (Yatavelli et al., 2017a) where SD ranged between 9.7 and 22%  
280 for methoxyphenol derivatives.

281



282 Methoxyphenols are key compounds in BB smoke since they constitute from 20 to 40% of total  
283 identified organic aerosol mass (Hawthorne et al., 1989; Yee et al., 2013). For this reason, these  
284 compounds are considered potential markers for wood combustion (Schauer et al., 2001b) and  
285 have been used as probable biomarkers to determine human exposure to BB emissions (Simpson  
286 and Naeher, 2010; Dills et al., 2006). Our analysis of 13 methoxyphenols (Fig. 2a, Table S1)  
287 showed that guaiacol (MW =  $124 \pm 12$  g mol<sup>-1</sup>) was the major contributor to EFs of the measured  
288 methoxyphenols in Moscow peat ( $33.5 \pm 3.3$  mg kg<sup>-1</sup>), Pskov peat ( $49.7 \pm 4.8$  mg kg<sup>-1</sup>), and  
289 Malaysian peat ( $68.6 \pm 6.7$  mg kg<sup>-1</sup>). Syringol, another methoxyphenol commonly found in BB  
290 emissions (Schauer et al., 2001a), had the highest EF for Moscow Peat fresh emissions ( $20.4 \pm 2.7$   
291 mg kg<sup>-1</sup>), while for the other fuels, the EF was much lower ( $0$ – $5.5$  mg kg<sup>-1</sup>). EFs for syringic acids  
292 (MW =  $198$  g mol<sup>-1</sup>) were in the range of  $0.06$ – $37.9$  mg kg<sup>-1</sup> for all fresh emissions. Syringols are  
293 generally not formed during pyrolysis of coniferous lignin, but during pyrolysis of deciduous  
294 lignin, where both guaiacols and syringols are formed (Mazzoleni et al., 2007). Presence of both  
295 guaiacol and syringol moieties in fresh emissions indicates that the part of the plant material that  
296 was responsible for peat formation was probably from deciduous trees, and this signature of  
297 deciduous trees from peat burning emission is irrespective of geographical origin of those peats  
298 (also shown by Schauer et al., 2001a). Acetovanillone, vanillin, and vanillic acid also were  
299 observed in fresh emissions with high abundance ( $5$ – $50$  mg kg<sup>-1</sup>). For example, vanillin is an  
300 abundant methoxyphenol in the fresh emissions from Pskov peat ( $46.7 \pm 5.4$  mg kg<sup>-1</sup>) which  
301 contributed 4.4% of the total mass of the 84 analyzed compounds.

302

303 Low molecular weight methoxyphenols (e.g., guaiacol) are expected to be found in the gas phase  
304 (Yatavelli et al., 2017b), in close agreement with our results. For example, guaiacol and substituted  
305 guaiacols were mostly present in gas phase ( $82$ – $100\%$ ) for emissions from the combustion of  
306 different fuels (Fig. 2a, Table S1). With the addition of more oxygenated functional groups to a  
307 molecule, and thus with molecular weight increase, the equilibrium gas-particle partitioning of the  
308 compound tends to shift toward the particulate phase, which also was confirmed by our results  
309 (e.g., for acetovanillone, a keto form of lignin derivative, from Malaysian peat combustion,  $33.5\%$   
310 of its mass was found in gas phase; for more oxygenated syringic acid,  $99\%$  of its mass was found  
311 in particulate phase emissions from the same fuel).



312

313 The highest methoxyphenol  $EF_{\text{group}}$  from combustion of all fuels was observed in the fresh Pskov  
314 peat (Fig. 3a) emissions ( $239 \pm 11 \text{ mg kg}^{-1}$ ). For Moscow peat, which was sampled close to the  
315 geographical region of Pskov peat, the  $EF_{\text{group}}$  of methoxyphenols was  $229 \pm 10 \text{ mg kg}^{-1}$  (Fig. 3a),  
316 very similar to that for Pskov peat. The methoxyphenol  $EF_{\text{group}}$  for peat samples were in the range  
317 of 66 to  $239 \text{ mg kg}^{-1}$  (Fig. 3a) for our 13 analyzed compounds. A previous study analyzed for 30  
318 different compounds (Schauer et al., 2001a) and consequently found a larger value  $EF_{\text{group}}$  of up  
319 to  $1330 \text{ mg kg}^{-1}$ , at least partially a result of the larger number of compounds analyzed. Formation  
320 of methoxyphenols during biomass combustion is mainly because of pyrolysis of lignin (e.g.,  
321 Simonelt et al., 1993). Lignin, an essential biopolymer of wood tissue, is primarily derived from  
322 three aromatic alcohols: p-coumaryl, coniferyl, and sinapyl alcohols (Hedges and Ertel, 1982).  
323 Lignins of hardwoods (angiosperms) are enriched with products from sinapyl alcohol; softwoods  
324 (gymnosperms) instead have a high proportion of products from coniferyl alcohol with a minor  
325 contribution from sinapyl alcohol; grasses have mainly products from p-coumaryl alcohol. The  
326 relative proportions of these bio-monomers vary considerably among the major plant classes  
327 (Sarkanen and Ludwig, 1971), reflected in our total emission factors estimate for 13  
328 methoxyphenols.

329

330

331

332

333

334

335

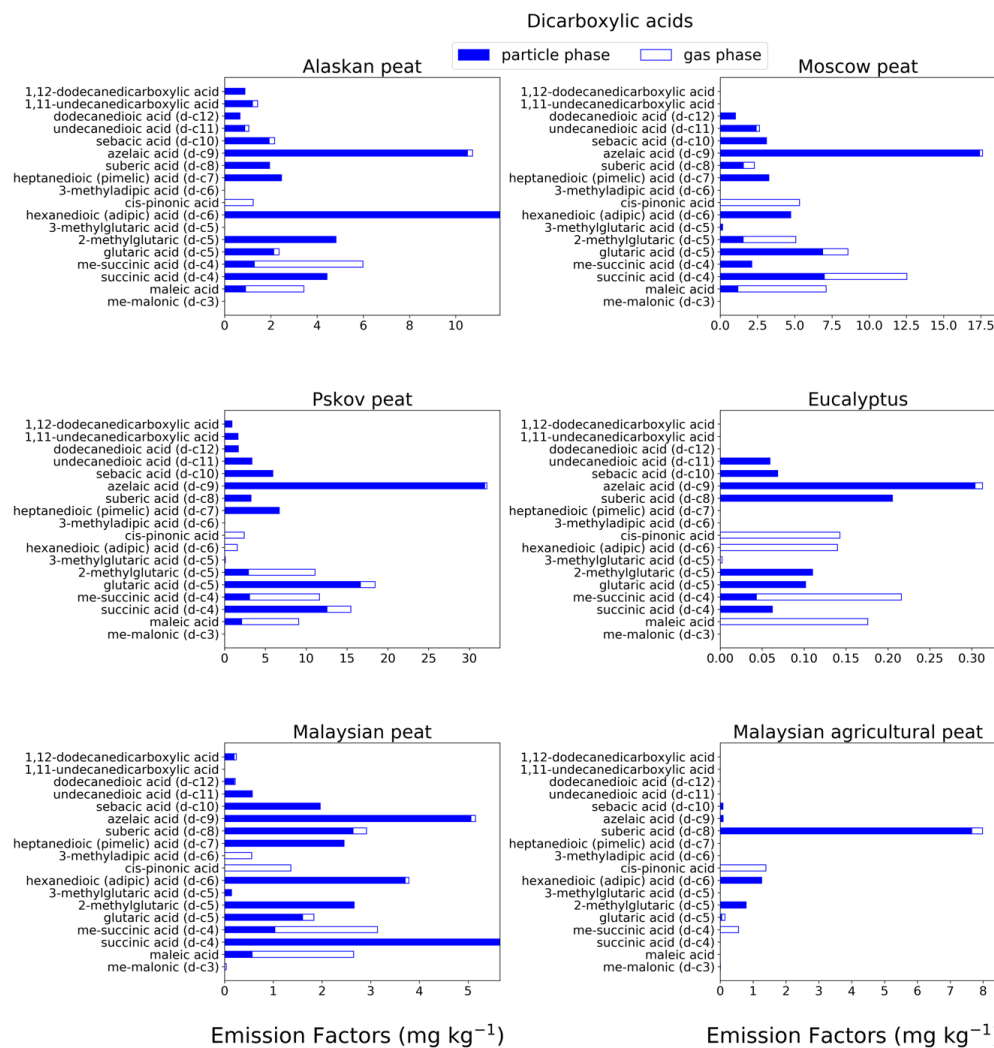
336

337

338



339 3.1.2 Dicarboxylic Acids



340

341 Figure 2b. EFs for dicarboxylic acids in both particulate phase (solid bars, filter samples) and gas-  
 342 phase (open bars, XAD samples) from fresh biomass-burning emissions for six different fuel types.  
 343 We did not burn fuels in replicates, and standard deviations (SD) were calculated based on replicate  
 344 analysis of emissions from similar fuels (with identical experimental conditions) during our  
 345 previous combustion campaigns (Yatavelli et al., 2017a) where SD ranged between 10 and 17%  
 346 for dicarboxylic acids.

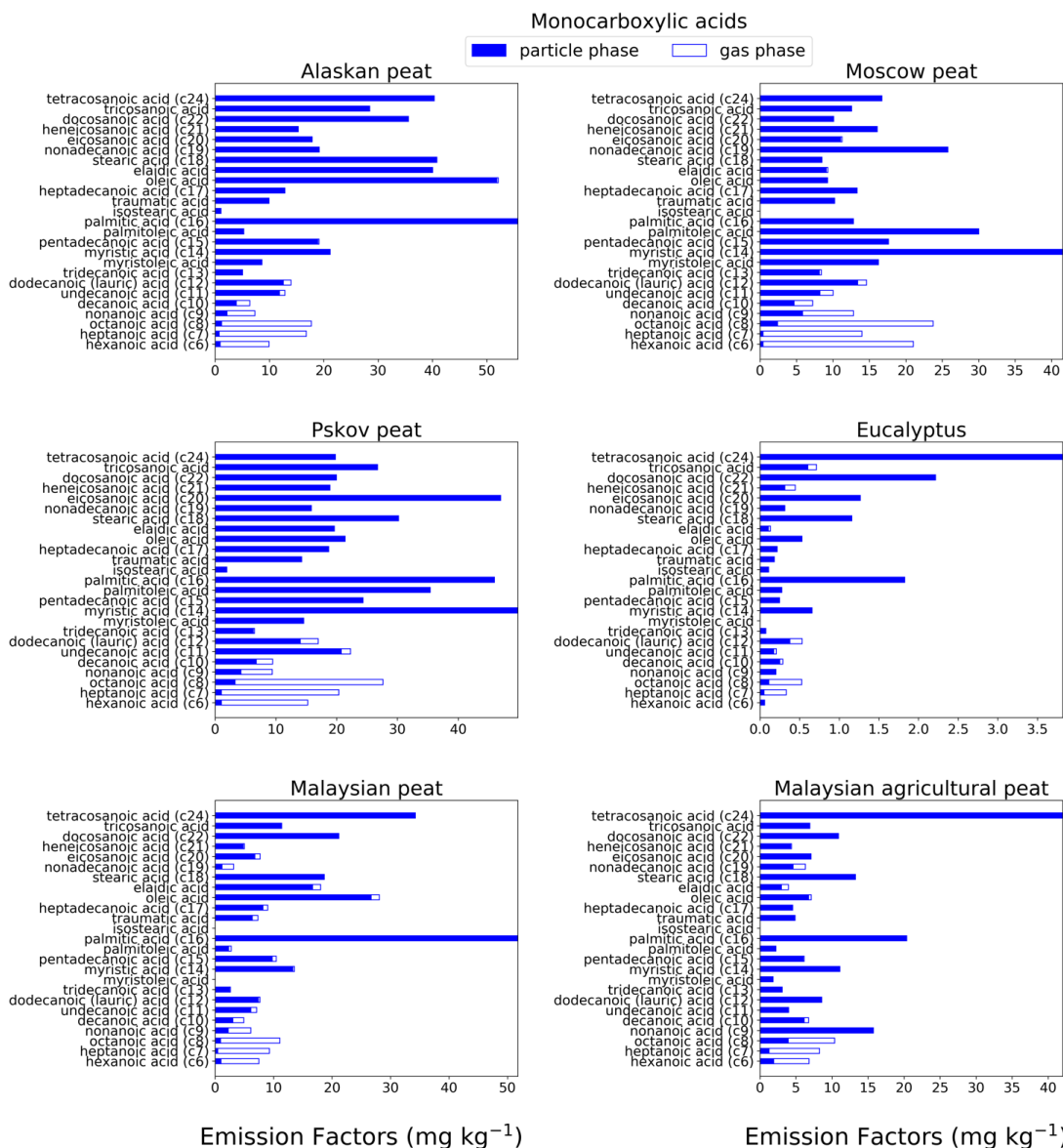


347

348 Dicarboxylic acids play a significant role in the atmospheric organic aerosols budget (Samburova  
349 et al., 2013; Yatavelli et al., 2017b) via secondary organic aerosol formation that either changes  
350 radiative forcing directly, or indirectly by acting as cloud condensation nuclei (Kawamura and  
351 Bikkina, 2016). The  $EF_{\text{group}}$  for dicarboxylic acids (Fig. 3b) varied among the fuels with the highest  
352  $EF$  for fresh Pskov peat samples ( $123 \pm 10 \text{ mg kg}^{-1}$ ) and with the lowest for Eucalyptus ( $1.5 \pm 0.1$   
353  $\text{mg kg}^{-1}$ ). This range in  $EF$ s can be attributed to difference in fuel type and burning conditions  
354 (smoldering vs. flaming). We also observed, however, a difference in the  $EF_{\text{group}}$  of dicarboxylic  
355 acid between two tropical peats from the same geographical area (Malaysian peat:  $EF = 35.33 \pm 2.9$   
356  $\text{mg kg}^{-1}$  and Malaysian agricultural peat:  $12.29 \pm 1.02 \text{ mg kg}^{-1}$ ). The highest  $EF$  for individual  
357 dicarboxylic acids was observed for azelaic acid. For example, for Pskov peat the  $EF$  was  $32.1 \pm 4.1$   
358  $\text{mg kg}^{-1}$ ; and for Moscow peat it, was  $17.6 \pm 2.6 \text{ mg kg}^{-1}$ . Azelaic acids were mostly found in the  
359 particulate phase (Fig. 2b, Table S1) and their relative abundances in the gas phase varied between  
360 0.77% (for Pskov peat) and 2.85% (for Eucalyptus. Maleic acid was mostly found in the gas phase  
361 (73%–83%), since it is a lower MW compound ( $MW = 116.0 \text{ g mol}^{-1}$ ) compared to azelaic  
362 ( $MW = 188.22 \text{ g mol}^{-1}$ ) and adipic ( $146.14 \text{ g mol}^{-1}$ ) acids. Succinic and methyl-succinic acids are  
363 found in both gas and particulate phases (Table S1), and their abundance in the particulate phase  
364 was 19–59% and 53–100%, respectively. For Malaysian peat BB emissions, succinic acid was  
365 present only in the particulate phase. A distinguishable increase in dicarboxylic acid mass  
366 concentrations was observed for ambient aerosols followed by a biomass burning event (Cao et  
367 al., 2017) compared to normal ambient concentrations. The formation of saturated dicarboxylic  
368 acids (e.g., succinic acid) and unsaturated dicarboxylic acids (e.g., maleic acid) also was reported  
369 for ambient aerosols collected near a biomass-burning event (Graham et al., 2002; Kundu et al.,  
370 2010; Zhu et al., 2018) and in ice core records historically affected by biomass burning (Müller-  
371 Tautges et al., 2016).



372 3.1.3 Monocarboxylic Acids



373

374 Figure 2c. EFs for monocarboxylic acids in both particulate phase (solid bars, filter samples) and  
 375 gas-phase (open bars, XAD samples) from fresh biomass burning emissions for six different fuel  
 376 types. We did not burn fuels in replicates and standard deviations (SD) were calculated based on





377 replicate analysis of emissions from similar fuels (with identical experimental conditions) during  
378 our previous combustion campaigns (Yatavelli et al., 2017a) where SD ranged between 9.4 and  
379 12% for monocarboxylic acids.

380

381 Monocarboxylic acids can constitute up to 30–40% of total identified organic aerosol mass from  
382 BB emissions (Oros et al., 2006). In our study, we characterized the range from C<sub>6</sub>–C<sub>24</sub>, where  
383 some unsaturated monocarboxylic acids (e.g., oleic acid) also are included. For Alaskan and  
384 Malaysian peat fresh emissions (Fig. 2c), the highest EF (gas + particle) among all analysed  
385 monocarboxylic acids was for hexadecanoic acid (C<sub>16</sub>) with EFs of 55.7±6.6 mg kg<sup>-1</sup> and 51.8±6.2  
386 mg kg<sup>-1</sup>, respectively. The dominance of hexadecanoic acid among other monocarboxylic acids in  
387 combustion emissions also was observed in ambient measurements during biomass-burning events  
388 in southeast Asia (Fang et al., 1999). For Moscow (41.5±6.5 mg kg<sup>-1</sup>) and Pskov (49.8±7.8 mg kg<sup>-1</sup>)  
389 peats, tetradecanoic acid (C<sub>14</sub>) had the highest EFs in fresh samples (Fig. 2c). For Eucalyptus  
390 and Malaysian agricultural peat fresh samples, the largest contributor to monocarboxylic acids was  
391 tetracosanoic acid (C<sub>24</sub>) (Fig. 2c) with EFs of 3.81±0.5 mg kg<sup>-1</sup> and 42.0±5.1 mg kg<sup>-1</sup>, respectively.  
392 As we expected, low molecular weight monocarboxylic acids like hexanoic acid (MW=116 g mol<sup>-1</sup>)  
393 was mostly present in the gas phase, and the gas phase mass fraction varied between 72% (for  
394 Malaysian agricultural peat) and 98% (for Moscow peat). Similar trends were observed for other  
395 low molecular weight monocarboxylic acids. For example, the relative abundance of octanoic acid  
396 (C<sub>8</sub>) in the gas phase was 93.4% for Alaskan peat. High molecular weight monocarboxylic acids  
397 (C<sub>16</sub>>) abundance in the gas phase was < 2% for all analyzed fuels.

398

399 Carbon preference index (CPI) is generally used for source apportionment of organic aerosols  
400 (Fang et al., 1999). We also computed the carbon preference index for monocarboxylic acids from  
401 all analyzed fuel combustion emissions by taking even carbon number over odd carbon number  
402 ratio on EFs of monocarboxylic acids ranges from C<sub>6</sub> to C<sub>24</sub> (Fig. S1). For fresh emission samples,  
403 the CPI values ranged from 1.28 (for Moscow peat) to 4.53 (for eucalyptus). The CPI values are  
404 higher for fresh emissions of tropical peats (for example, 2.78 for Malaysian peat) than for  
405 emissions from peats from high latitudes (for example, 1.74 for Pskov peat). An average CPI index  
406 of 3.7 for monocarboxylic acids was reported for combustion emissions from sedimentary bogs



407 (Freimuth et al., 2019), in the range of our reported values (CPI: 1.3–4.5).

408

409 The sums of the EFs for 25 monocarboxylic acids are shown in Fig. 3c. The  $EF_{\text{group}}$  was in the  
410 range of 5 and 515  $\text{mg kg}^{-1}$  for all fuels. This range is comparable to the  $EF_{\text{group}}$  reported previously  
411 for grass (tundra, cotton, Pampas and ryegrass) combustion (32–250  $\text{mg kg}^{-1}$ ) (Oros et al., 2006).  
412 Overall, the trend of low EFs associated with flaming combustion of Eucalyptus ( $16 \pm 0.7 \text{ mg kg}^{-1}$ )  
413 compared to smoldering peat combustion is also evident for this compound category. Combustion  
414 of peat fuels from tropical regions (e.g., Malaysian agricultural peat) resulted in monocarboxylic  
415 acids EFs of  $212 \pm 9.6 \text{ mg kg}^{-1}$  compared to higher EFs from Alaskan peat combustion ( $505 \pm 23 \text{ mg}$   
416  $\text{kg}^{-1}$ ). The origin of monocarboxylic acid is mostly plant wax and oils (Simoneit, 2002). The  
417 relative proportion of plant wax and oils can vary widely among vegetation taxa and also their  
418 concentrations in peat depend on biogeochemical processes involved in peat formation. The  
419 differences in relative abundance of waxes and plant oils in living vegetation and the differences  
420 between biogeochemical processes involved in peat formation for arctic and tropical regions may  
421 be responsible for diverse EFs for monocarboxylic acids.

422

423

424

425

426

427

428

429

430

431

432

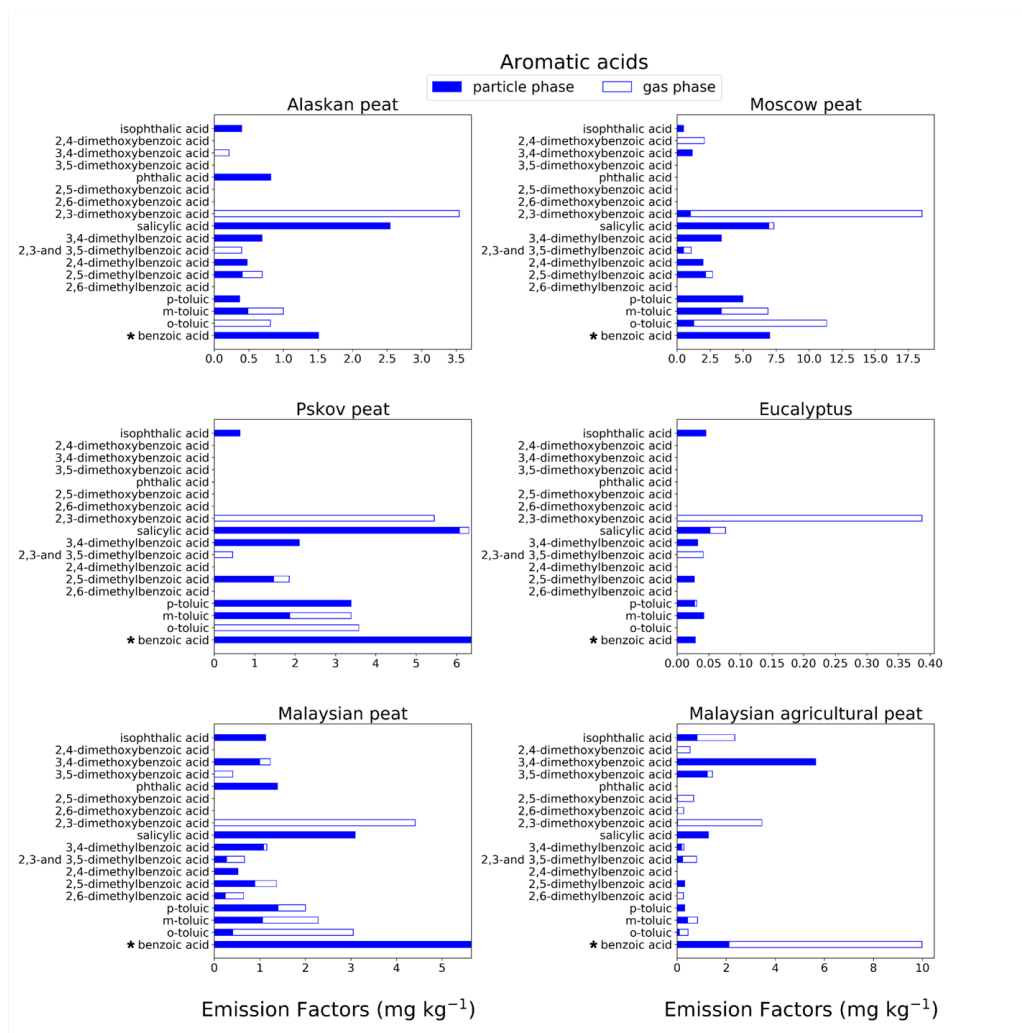
433

434

435



436 3.1.4 Aromatic Acids



437  
438 Figure 2d. EFs for aromatic acids in both particulate phase (solid bars, filter samples) and gas-  
439 phase (open bars, XAD samples) from fresh biomass burning emissions for six different fuel types.  
440 We did not burn fuels in replicates, and SD were calculated based on replicate analysis of  
441 emissions from similar fuels (with identical experimental conditions) during our previous  
442 combustion campaigns (Yatavelli et al., 2017a) where SD ranged between 9.5 and 15% for  
443 aromatic acids; \*Benzoic acid was found in high concentrations in the XAD blanks that introduced  
444 a substantial uncertainty to quantification of this compound.



445

446 Aromatic acids from BB emissions can contribute up to 20–35 % of total identified organic mass  
447 (Wan et al., 2019). In our study, the aromatic acids (e.g., p-hydroxy benzoic acid), excluded  
448 methoxyphenol derivatives and resin acids. For most of the fuels, LMW aromatic acids (MW <150  
449 g mol<sup>-1</sup>) (e.g., benzoic acid, o-/m-/p-toluic acids) contributed more (almost 40% of total aromatic  
450 acid emissions) toward total fresh emissions, compared to HMW aromatic acids (MW >150 g mol<sup>-1</sup>).  
451 For example, the benzoic acid EF for Malaysian agricultural peat fresh emission (Fig. 2d) is  
452 9.98±1 mg kg<sup>-1</sup>, and the EF for the same benzoic acid is 6.36±0.6 mg kg<sup>-1</sup> for Pskov peat (Fig. 2d).  
453 Although, o-toluic and p-toluic acids are found in gas phase with 50%–100% abundance in  
454 Alaskan and Moscow peat, benzoic acid is found only in particulate phase. Benzoic acid was found  
455 in high concentrations in the XAD blanks that introduced a substantial uncertainty to quantification  
456 of this compound. One of the most abundant aromatic acids in fresh peat emissions was 2,3-  
457 dimethoxy benzoic acid. For example in Moscow peat, the EF was 18.6±4.7 mg kg<sup>-1</sup>. The acid was  
458 mostly found in gas phase (91%–100%) for all fuels (Fig. 2d, Table S1). 2,3-dimethoxy benzoic  
459 acid is potentially derived from combustion of lignin moieties of biomass, and the emission of this  
460 compound is more than an order of magnitude lower in emissions from flaming combustion  
461 samples (EF=0.38 ±0.09 mg kg<sup>-1</sup>) than in emissions from smoldering combustion emissions  
462 (EF=5.44±1.36 mg kg<sup>-1</sup>). Emissions of 3,4 dimethoxy benzoic acid were only observed for peats  
463 from tropical regions (EF=5.64±0.8 mg kg<sup>-1</sup>) with 80–100% abundance in particulate phase. This  
464 compound can be used for source apportionment of aerosols emitted from burning of tropical peat  
465 and also can potentially help to distinguish between emissions from tropical and high latitude  
466 peatland fires.

467

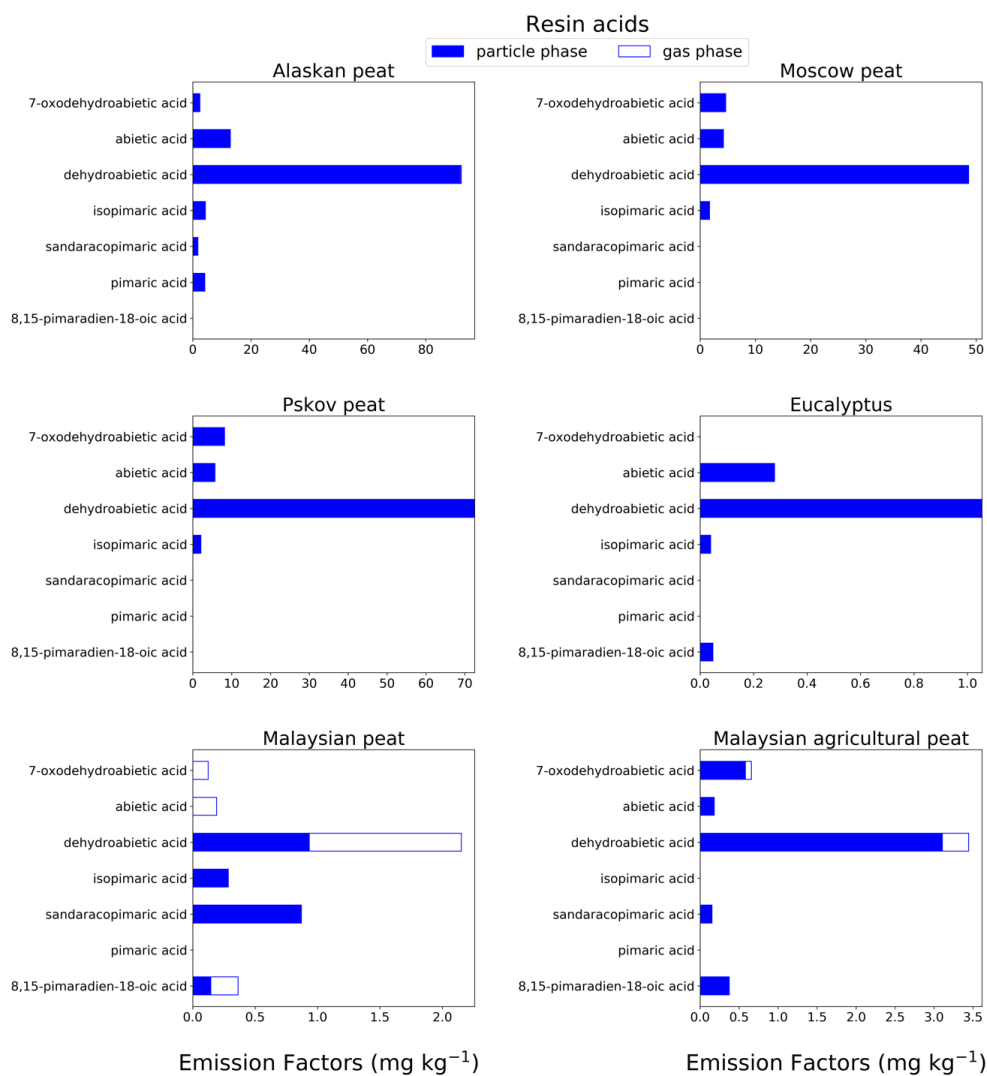
468 The EF<sub>group</sub> for aromatic acids in fresh combustion emissions from eucalyptus fuel is extremely  
469 low (0.71±0.05 mg kg<sup>-1</sup>) compared to that for peat fuels (13–69 mg kg<sup>-1</sup>). Among all peat samples,  
470 the Alaskan peat fresh EF was the lowest EF (13.5±0.9 mg kg<sup>-1</sup>), whereas Moscow peat fresh  
471 emissions yielded the highest EF (69±4.4 mg kg<sup>-1</sup>). The difference in total aromatic acid emissions  
472 can be attributed to the variation in the lignin content of the fuels and burning conditions (Simoneit,  
473 2002).

474



475

### 476 3.1.5 Resin Acids



477

478 Figure 2e. EFs of resin acids in both particulate phase (solid bars, filter samples) and gas-phase  
479 (open bars, XAD samples) from fresh biomass-burning emissions for six different biomass types.  
480 As in prior cases, we did not burn fuels in replicates, and SD were calculated based on replicate  
481 analysis of similar fuels (with same experimental conditions) from our previous campaigns



482 (Yatavelli et al., 2017a) and SD varies from 9.7–15% for resin acids  
483 We quantitatively analyzed combustion emissions for isomers in six resin acids (Table S1). The  
484 most abundant resin acid (78% of total resin acid emission) is dehydroabietic acid (C<sub>20</sub>) that does  
485 not have isomers. The preponderance of this acid over other resin acids in emissions from oak and  
486 pine biomass burning was reported by Simoneit et al. (1993). We found that dehydroabietic acid  
487 (C<sub>20</sub>) content in fresh emissions is 15–30 times higher in fuels from high-latitude peatlands than in  
488 those of tropical origin. For example, the EF for dehydroabietic acid in fresh Alaskan peat  
489 emissions is 92.2±14 mg kg<sup>-1</sup> (Fig. 2e), whereas the same in fresh Malaysian peat emissions is  
490 3.44±0.5 mg kg<sup>-1</sup> (Fig. 2e). Resin acids are supposed to be found mostly in particulate phase based  
491 on their molecular weight and functional groups (Asher et al., 2002; Pankow and Asher,  
492 2008)(Karlberg et al., 1988), confirmed by our results (80–100% in particulate phase) with the  
493 exception of Malaysian peat emissions where 56.6% abundance of dehydroabietic acid was found  
494 in gas phase. Although a distinct peak of dehydroabietic acid was observed at the desired retention  
495 time for this sample during GC-MS analysis, we believe this result can be attributed to some  
496 unknown interference from our analysis procedure.

497

498 The EF<sub>group</sub> for seven resin acids are presented in Fig. 3e. High EF<sub>group</sub> was observed for Alaskan  
499 (117±15 mg kg<sup>-1</sup>), Pskov (89±12 mg kg<sup>-1</sup>), and Moscow (59±7.7 mg kg<sup>-1</sup>) peats representing mid  
500 latitude and arctic peats. Resin acids (e.g., pimaric acid) are biosynthesized mainly by conifers  
501 (gymnosperms) in temperate regions. In previous work, Iinuma et al. (2007) gave a range of resin  
502 acids EFs from 0 to 110 mg kg<sup>-1</sup>, in agreement with our results. Very low resin acids EFs were  
503 found for peat from tropical regions (e.g., 4 mg kg<sup>-1</sup> for Malaysian peat fresh samples). As  
504 deciduous trees in tropical zones are not prolific resin and mucilage (gum) producers,  
505 compositional data on smoke from such sources should not be expected to show moderate  
506 concentrations of resin acids. This is supported by earlier work by Iinuma et al. (2007), where resin  
507 acids were not even detectable for emissions from Indonesian peat combustion.

508



509 **3.1.5 Levoglucosan**

510 Levoglucosan can be found mostly in particulate phase (Simoneit, 2002). We report levoglucosan  
511 EFs from our analysis of the quartz filter using the IC-PAD technique (no gas phase EFs reported).  
512 The EFs of levoglucosan (Fig. 3f) were found to be  $20.9 \pm 0.68 \text{ mg kg}^{-1}$  and  $485 \pm 11.8 \text{ mg kg}^{-1}$  for  
513 Eucalyptus and Malaysian peat, respectively, and their carbon content is approximately 1.8% and  
514 2.5 % of the total organic carbon mass characterized by the thermo-optical technique. Fine et al.  
515 (2002) reported 9% to 16% contribution of levoglucosan to total OC from residential wood  
516 combustion, a relatively higher percentage than values obtained in our study. Anhydrosugars (e.g.,  
517 levoglucosan and its isomers) are found in great abundance and have been widely used as a BB  
518 tracer because of their atmospheric stability, as summarized by Bhattarai et al. (2019). We found  
519 that levoglucosan constituted 36% and 51% of GC-MS characterized polar (listed in our method)  
520 organic aerosol mass for eucalyptus and Malaysian peat, respectively, which also is consistent with  
521 the previous BB literature assembled in the recent review article by Bhattarai et al. (2019).

522

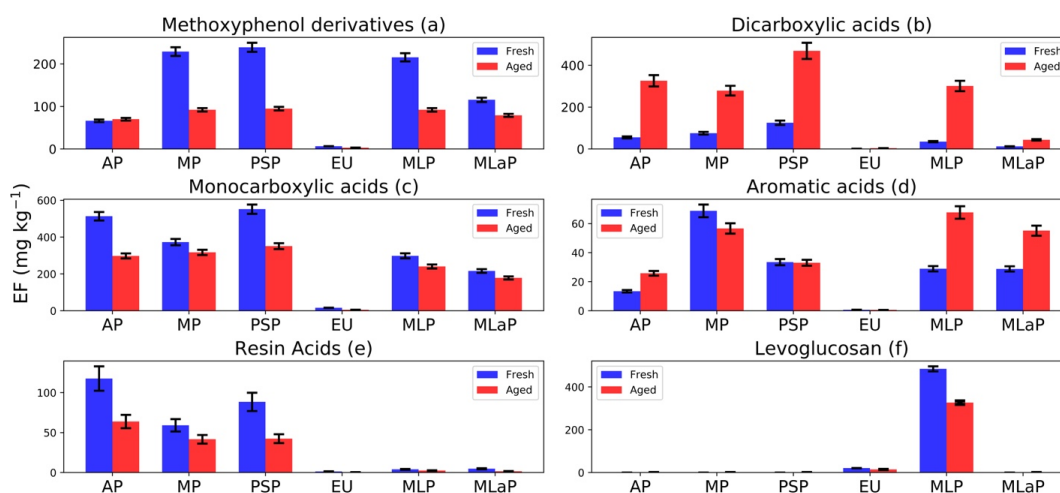
523



524 **3.2. Emission factors of total (gas + particle) organic compounds of six chemical groups and**  
525 **their changes upon OFR oxidations**

526

527 Here we describe changes in the  $EF_{\text{group}}$  followed by OFR oxidation for all six chemical groups.  
528 Levoglucosan and the most abundant resin acid, dehydroabietic acid also are reported in this  
529 section.



530

531 Figure 3. Fuel-based emission factors (EFs) of organic compounds assigned to six chemical groups  
532 for six different fuels: Alaskan peat (AP), Moscow peat (MP), Pskov peat (PSP), Eucalyptus (EU),  
533 Malaysian peat (MLP), Malaysian agricultural peat (MLaP). EFs are presented as a sum of gas-  
534 and particle-phase species mass measured in fresh and OFR-aged BB emissions in units of  $\text{mg kg}^{-1}$   
535 (mass of emissions per fuel mass combusted). We did not burn fuels in replicates, and standard  
536 deviations (SD) of all chemical groups were calculated based on replicate analysis of similar fuels  
537 (with same experimental conditions) from our previous campaign based on the data reported by  
538 Yatavelli et al. (2017).

539

540 *3.2.1. Methoxyphenol derivatives after OFR oxidation (Fig. 3a)*

541 Methoxyphenols can undergo gas-phase oxidation reactions via either aromatic ring  
542 fragmentation/opening to form short-chain ketones, acids, esters, and double bonds in conjugations





543 with all functional groups or further hydroxylation of aromatic rings to form multiple substituted  
544 aromatic compounds (Yee et al., 2013). In either case, a decrease in methoxyphenols after  
545 oxidation was expected. In our study, a decrease in methoxyphenol's  $EF_{\text{group}}$  with OFR oxidations  
546 were observed for all fuels (e.g., for Pskov peat from  $239 \pm 11 \text{ mg kg}^{-1}$  to  $95 \pm 4 \text{ mg kg}^{-1}$ ) except for  
547 Alaskan peat, where an insignificant increase from  $66 \pm 3 \text{ mg kg}^{-1}$  to  $70 \pm 3 \text{ mg kg}^{-1}$  after the OFR  
548 oxidation was observed.

549

### 550 3.2.2. Dicarboxylic acid group after OFR oxidation (Fig. 3b)

551 A significant increase (2.5–8.5 times) in the  $EF_{\text{group}}$  of dicarboxylic acids was observed for OFR-  
552 aged samples. For example, the  $EF_{\text{group}}$  of dicarboxylic acids increased from  $35 \pm 3 \text{ mg kg}^{-1}$  to  
553  $301 \pm 25 \text{ mg kg}^{-1}$  for Malaysian peat and from  $56 \pm 5 \text{ mg kg}^{-1}$  to  $326 \pm 27 \text{ mg kg}^{-1}$  for Alaskan peat.  
554 Oxidation of aerosols potentially produces more oxygenated functional groups (Jimenez et al.,  
555 2009), demonstrated by an increase in O:C ratios (from 0.45 to 0.65) in recent laboratory oxidation  
556 of BB emissions by Bertrand et al. (2018), where TAG-AMS was used to identify the fate of  
557 organic compounds. In this work, however, the number of identifiable compounds with highly  
558 functional groups is constrained by the elution technique used in the TAG method. Our results on  
559 the fate of BB organic aerosols with 18 dicarboxylic acids can provide better mechanistic  
560 understanding about the processes inside OFR.

561

### 562 3.2.3. Monocarboxylic acid group after OFR oxidation (Fig. 3c)

563 We observed a decrease in monocarboxylic acids  $EF_{\text{group}}$  from OFR aging for all fuels. For  
564 example, the  $EF_{\text{group}}$  for monocarboxylic acids from Alaskan peat combustion decreased from  
565  $514 \pm 23 \text{ mg kg}^{-1}$  (fresh) to  $298 \pm 14 \text{ mg kg}^{-1}$  (aged). A relatively small decrease compared to Alaskan  
566 peat was observed for Malaysian agricultural peat (from  $216 \pm 10 \text{ mg kg}^{-1}$  [fresh] to  $179 \pm 8 \text{ mg kg}^{-1}$   
567 [aged]) and Malaysian peat (from  $298 \pm 14 \text{ mg kg}^{-1}$  [fresh] to  $240 \pm 11 \text{ mg kg}^{-1}$  [aged]) too. This is  
568 probably because of the formation of low molecular weight (LMW) monocarboxylic acids (e.g.,  
569 hexanoic acids;  $MW=116 \text{ g mol}^{-1}$ ) after OFR oxidation demonstrated in Fig. 4c and Table S2c and  
570 will be discussed further in section 3.3. Monocarboxylic acids can be oxidized in the atmosphere  
571 (Charbouillot et al., 2012), leading to the formation of dicarboxylic acids from  $C_2$  to  $C_6$  (Ervens et



572 al., 2004). This is consistent with our results (Figs. 3b, 3c, Table S2b) Moreover, monocarboxylic  
573 acids, during their atmospheric transformations, can produce a potential precursor for formation  
574 of high molecular weight compounds, such as Humic Like Substance (HULIS) (Carlton et al.,  
575 2007; Tan et al., 2012).

576

#### 577 3.2.4. Aromatic acid group after OFR oxidation (Fig. 3d)

578 Levels of aromatic acids from peat burning increased for Alaskan peat, Malaysian peat, and  
579 Malaysian agricultural peat (e.g., from  $29\pm 2$  mg kg<sup>-1</sup> to  $68\pm 4$  mg kg<sup>-1</sup> for Malaysian peat) by OFR  
580 aging (Fig. 3e, Table S2e). This increase could be from oxidation of phenols and methoxyphenols  
581 in the OFR chamber (Akagi et al., 2011b; Legrand et al., 2016). For eucalyptus, Moscow and  
582 Pskov peats it was an insignificantly small decrease (e.g., from  $69\pm 4$  mg kg<sup>-1</sup> to  $57\pm 3$  mg kg<sup>-1</sup> for  
583 Moscow peat and from  $34\pm 2$  mg kg<sup>-1</sup> to  $33\pm 2$  mg kg<sup>-1</sup> for Pskov peat). This small decrease in the  
584 EF<sub>group</sub> of monocarboxylic acids is statistically insignificant. The oxidation processes occurring in  
585 the OFR are complex, especially in the case of multi-component BB emissions. The decrease  
586 observed for aromatic acids after the OFR may be attributed, however, to multiple generations of  
587 oxidation leading to the breaking of aromatic rings and formation of low molecular weight organic  
588 compounds via fragmentation (Jimenez et al., 2009).

589

590

#### 591 3.2.5. Resin acids after OFR oxidation (Figs. 3d and 4e)

592 Resin acids can be oxidized to corresponding oxo-acids (e.g., 7-oxodehydroabietic acid (Karlberg  
593 et al., 1988)), and they are considered to be stronger contact allergens than the resin acids  
594 themselves (Sadhra et al., 1998). Our data showed a small decrease in 7-oxodehydroabietic acid  
595 levels after the OFR (e.g., from  $8.2\pm 0.8$  to  $4.8\pm 0.5$  mg kg<sup>-1</sup> for Pskov peat). We noted a significant  
596 decrease in the EF<sub>group</sub> of resin acids from  $117\pm 15$  mg kg<sup>-1</sup> (fresh) and  $63\pm 8$  mg kg<sup>-1</sup> (aged) for  
597 Alaskan peat after OFR oxidation, mostly because of some individual compounds like  
598 dehydroabietic acid. Although resin acids are considered to be stable atmospheric tracers for  
599 biomass burning (Simoneit et al., 1993a), we observed a decrease in dehydroabietic acid (most  
600 abundant) EF after the OFR-oxidation of emissions from all fuels (Fig. S2b). For example, for



601 Alaskan peat (Fig. S2b), the decrease was from  $92 \pm 14 \text{ mg kg}^{-1}$  to  $57 \pm 8 \text{ mg kg}^{-1}$  after OFR-  
602 oxidation. The fate of resin acids during OFR aging, however, was beyond the scope of this work  
603 and may be the subject of future investigations.

604

### 605 3.2.6. Levoglucosan after OFR oxidation (Fig. 3f)

606 Levoglucosan is one of the most popular tracers of BB emissions, since it has been considered a  
607 stable compound in the atmosphere (Oros et al., 2006; Simoneit, 2002; Simoneit et al., 1999).  
608 Several laboratory studies, however, have demonstrated degradation of levoglucosan in the  
609 presence of OH radicals (Hennigan et al., 2010). Here we observed a decrease of 30% in  
610 levoglucosan levels following OFR oxidation. For example, Malaysian peat decreased from  
611  $485 \pm 12 \text{ mg kg}^{-1}$  to  $327 \pm 8 \text{ mg kg}^{-1}$ . For eucalyptus, the decrease was from  $20 \pm 0.7 \text{ mg kg}^{-1}$  to  $14 \pm 0.6$   
612  $\text{mg kg}^{-1}$ . This decrease also can be attributed to the degradation process during OH oxidation  
613 (Hoffmann et al., 2010). Levoglucosan oxidation should be studied more, so it can be adequately  
614 used as a tracer of BB emissions.

615



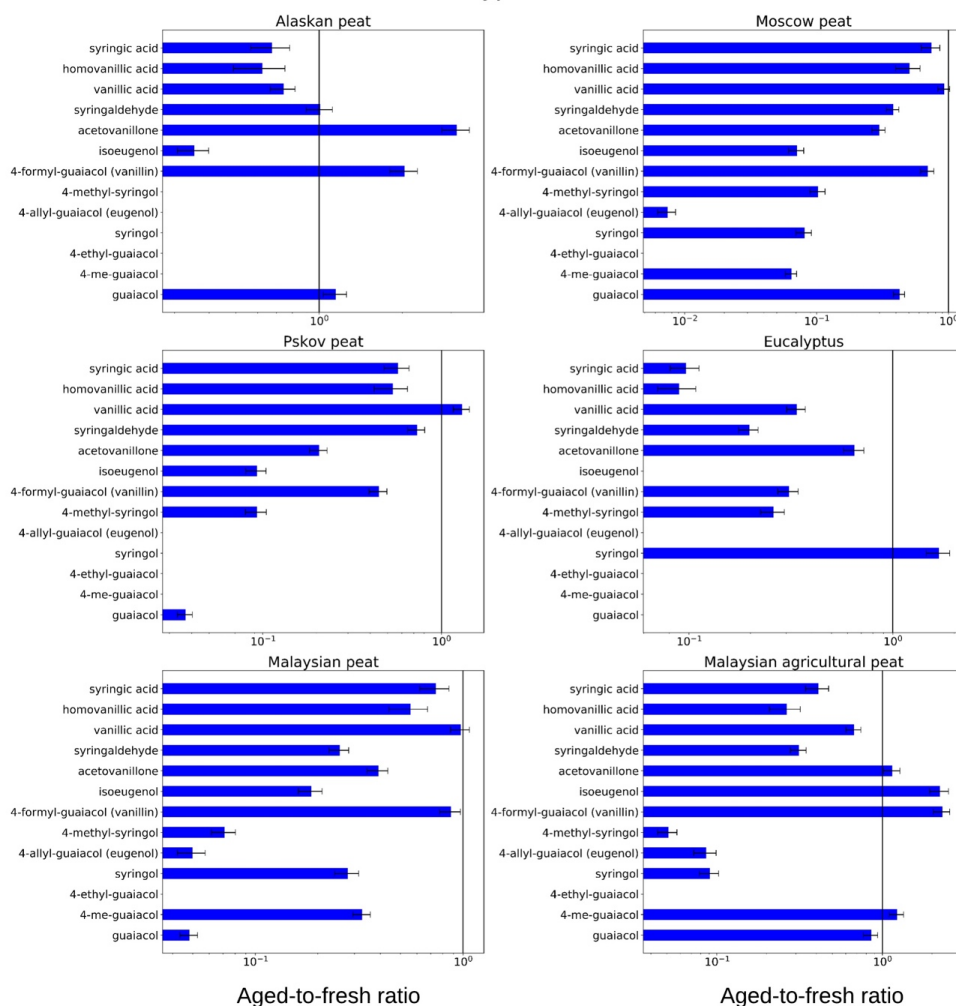
616 **3.3. Aged-to-fresh ratios of total (gas + particle) emission factors of individual organic**  
617 **compounds assigned to six chemical groups and their changes upon OFR oxidation**

618 We computed aged-to-fresh ratios of individual compounds for all fuels. If the aged-to-fresh ratio  
619 of one compound is greater than one, this implies that the compound is formed during OFR  
620 oxidations; if the ratio is less than one, then the compound must have decomposed inside the OFR.

621

622 **3.3.1 Methoxyphenol Derivatives**

Methoxyphenol derivatives



623



624 Figure 4a. Aged-to-fresh ratios of total (gas + particle) EFs for methoxyphenols from biomass  
625 burning emissions for six different biomass types presented in log scale. We did not burn fuels in  
626 replicates, and standard deviations (SD) were calculated based on replicate analysis of similar fuels  
627 (with same experimental conditions) from our previous campaigns. SD values derived from EFs  
628 were scaled to ratio.

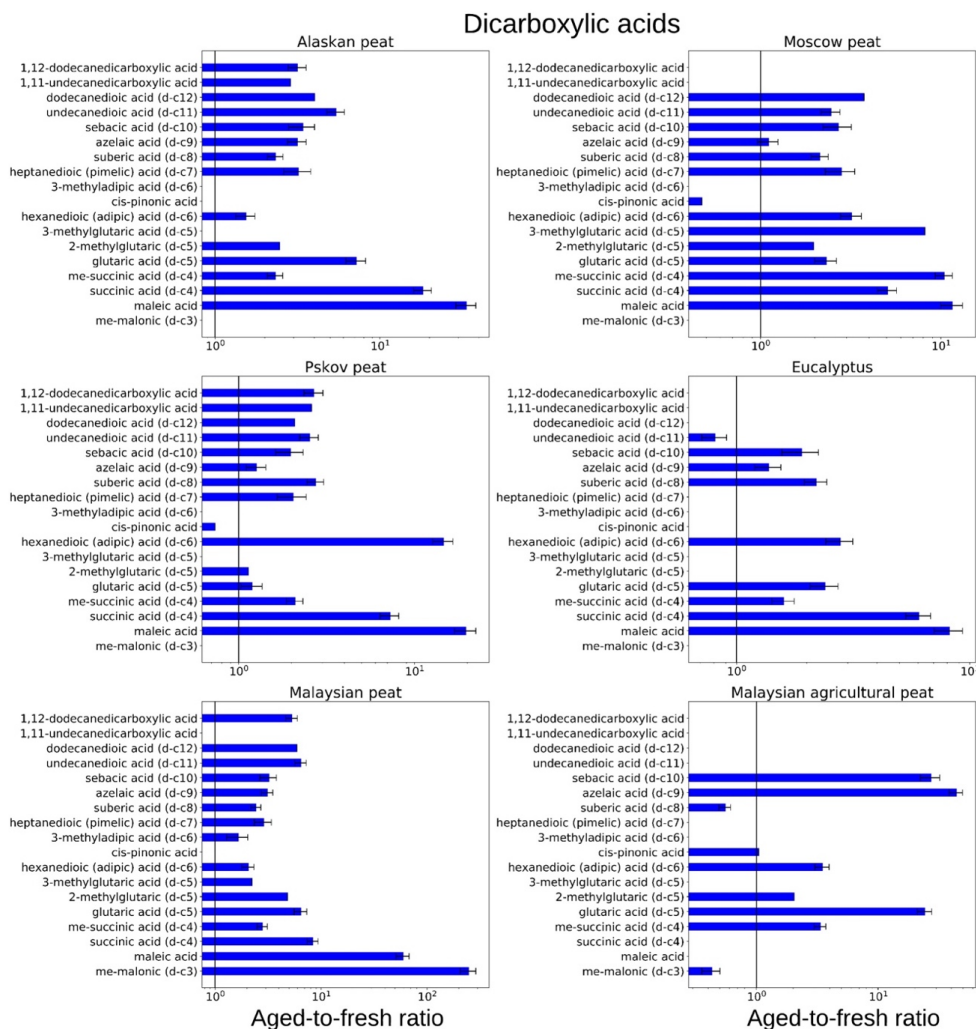
629

630 Overall, we found that abundances for methoxyphenol derivatives rapidly decreased upon OFR-  
631 oxidation (Fig. 4a, Table S2a). Some compounds—vanillic acid, acetovanillone, and syringic  
632 acids— demonstrated both increasing and decreasing trends. For example, for Pskov peat, the  
633 aged-to-fresh ratio of guaiacol was  $0.04 \pm 0.01$  reflecting a significant decrease during OFR  
634 oxidation. For Pskov peat, we also observed a ratio less than one for vanillin ( $0.44 \pm 0.05$ ),  
635 indicating vanillin also decreased during OFR oxidation for the same fuel but not to the extent of  
636 guaiacol. At the same time and for the same fuel, a slight increase (aged-to-fresh ratio  $>1$ ) in  
637 vanillic acid was observed ( $1.30 \pm 0.13$ ) in the OFR-oxidized sample. This increase in vanillic acid  
638 concentration can be attributed to the oxidation of vanillin, one of the abundant methoxyphenol in  
639 the fresh emissions from Pskov peat (Fig. 4a, Table S2a). For combustion of other peats, vanillic  
640 acid concentrations also decreased (e.g., aged-to-fresh ratios were  $0.74 \pm 0.08$  and  $0.67 \pm 0.07$  for  
641 Alaskan peat and Malaysian agricultural peat, respectively). Acetovanillone increased by a factor  
642 of three during OFR oxidation for Alaskan peat and around 15 % for Malaysian agricultural peat  
643 (aged-to-fresh ratio  $1.15 \pm 0.13$ ), but the increase for Malaysian agricultural peat was not  
644 statistically significant. For other fuels, acetovanillone decreased during the OFR oxidation. For  
645 example, for Moscow Peat, the aged-to-fresh ratio for acetovanillone was  $0.30 \pm 0.03$ . We still need  
646 to investigate the reason why both acetovanillone and vanillic acid increased for some fuels and  
647 decreased for others. The reduction of acetovanillone and vanillic acid was because of a photo-  
648 chemical decomposition process in the OFR with formation of lower molecular weight products,  
649 such as succinic acid and maleic acid (Schnitzler and Abbatt, 2018).

650



651 3.3.2 Dicarboxylic Acids



652

653 Figure 4b. Aged-to-fresh ratios of total (gas + particle) EFs for dicarboxylic acids from biomass  
 654 burning emissions for six different biomass types presented in log scale. We did not burn fuels in  
 655 replicates, and SD were calculated based on replicate analysis of similar fuels (with same  
 656 experimental conditions) from our previous campaigns. SD values derived from EFs were scaled  
 657 to ratio.

658



659 In the case of dicarboxylic acids, we observed 2–20 times increase in EFs, but the degree of  
660 enhancement of low-MW (LMW) dicarboxylic acids EFs was higher than for high-MW (HMW)  
661 dicarboxylic acids EFs. For example, a 20-fold increase in maleic acid, a LMW dicarboxylic acid  
662 (MW= 116.07 g mol<sup>-1</sup>), was observed during OFR oxidation of Pskov peat emissions (aged-to-  
663 fresh ratio = 19.6±2.8), whereas 1,11-undecanedicarboxylic acid, an HMW dicarboxylic acid  
664 (MW = 244.33 g mol<sup>-1</sup>), EF increased 2.6 times (aged-to-fresh ratio = 2.6±0.001) for the same fuel.  
665 Similarly, the concentration of succinic acid, an LMW dicarboxylic acid (MW= 118.09 g mol<sup>-1</sup>),  
666 increased almost by five times after OFR oxidation (aged-to-fresh ratio = 5.07±0.62), whereas that  
667 of undecanedioic acid, an HMW dicarboxylic acid (MW = 230.30 g mol<sup>-1</sup>), increased 2.5 times  
668 (aged-to-fresh ratio = 2.46±0.30) for Moscow peat. This trend was in accord with results from  
669 ambient observations after BB events (Cao et al., 2017; Kawamura and Bikkina, 2016).

670

671

672

673

674

675

676

677

678

679

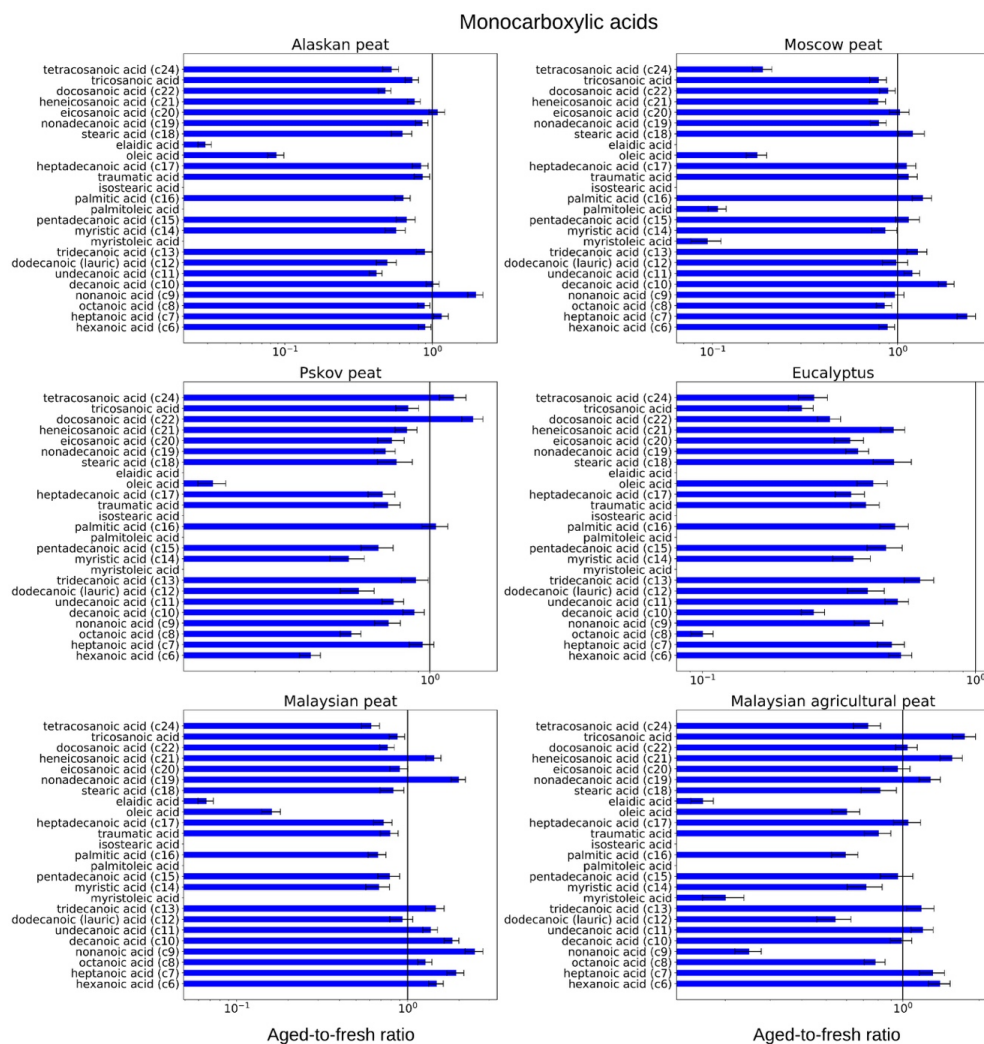
680

681

682



683 3.3.3 Monocarboxylic Acids



684

685 Figure 4c. Aged-to-fresh ratios of total (gas + particle) EFs for monocarboxylic acids from biomass  
686 burning emissions for six different biomass types presented in log scale. We did not burn fuels in  
687 replicates, and SD were calculated based on replicate analysis of similar fuels (with same  
688 experimental conditions) from our previous campaigns. SD values derived from EFs were scaled  
689 to ratio.

690





691 Our analysis of OFR-aged samples showed that concentrations of monocarboxylic acids with  
692 different molecular weights changed during OFR oxidation, but the changes varied from one fuel  
693 to another. For example, the EF of hexanoic acid ( $C_6$ ) was reduced for Eucalyptus (aged-to-fresh  
694 ratio =  $0.5 \pm 0.05$ ) and fuels from other high-latitude peatlands like Alaskan (aged-to-fresh ratio =  
695  $0.89 \pm 0.09$ ), Moscow (aged-to-fresh ratio =  $0.88 \pm 0.09$ ) and Pskov peat (aged-to-fresh ratio =  
696  $0.33 \pm 0.03$ ). The reduction of hexadecenoic acid was statistically insignificant for Alaskan and  
697 Moscow peat. The peats from tropical regions showed exactly the opposite change. Hexanoic acid  
698 increased for both Malaysian (aged-to-fresh ratio =  $1.47 \pm 0.14$ ) and Malaysian agricultural peat  
699 (aged- to-fresh ratio =  $1.40 \pm 0.14$ ). We observed a similar trend for heptanoic acid ( $C_7$ ) during OFR  
700 oxidation. The tropical peats clearly demonstrated increases (for example, aged-to-fresh ratio =  
701  $1.92 \pm 0.22$  for Malaysian peat) in heptanoic acid concentration. For Moscow peat, even though  
702 hexanoic acid concentrations were insignificantly decreased, heptanoic acid concentrations  
703 increased significantly (aged-to-fresh ratio =  $2.37 \pm 0.27$ ). This contrast between changes in  
704 hexanoic and heptanoic acid can be explained by a decrease in CPI indices during OFR oxidations  
705 (for example, from 2.78 to 1.7 for Malaysian peat). The reduction of CPI indices indicated that  
706 during oxidation more monocarboxylic acids with odd carbon numbers were formed than  
707 monocarboxylic acids with even carbon numbers. The abundance of hexadecenoic acid ( $C_{16}$ ) was  
708 reduced during OFR oxidation for all fuels (for example, aged-to-fresh ratio =  $0.63 \pm 0.08$  for  
709 Alaskan peat) except for Moscow and Pskov peat aged-to-fresh ratio =  $1.05 \pm 0.13$  for peat), and  
710 we believe this small increase is statistically insignificant. Similarly, tetracosanoic acid ( $C_{20}$ ) was  
711 reduced for all fuels (for example, aged-to-fresh ratio =  $0.61 \pm 0.07$  for Malaysian peat) except for  
712 Pskov peat (aged-to-fresh ratio =  $1.24 \pm 0.15$ ). The small increase in tetracosanoic acid ( $C_{20}$ )  
713 concentration was again statistically insignificant. Even though our results indicated the possibility  
714 of fragmentation of HMW monocarboxylic acids and formation of LMW monocarboxylic acids,  
715 this was because of the complexity of the OFR oxidation environment. We are not able to  
716 hypothesize what is the main reactive mechanism.

717

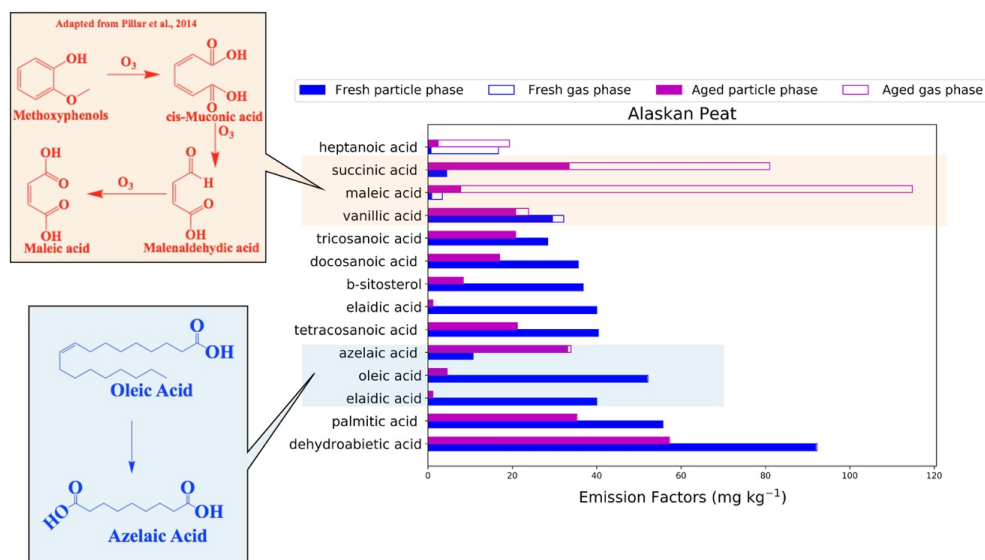
718

719

720



### 721 3.4. Most Contributing Compounds



722

723

724 Figure 5. Emission factors (EF) of top contributing organic compounds assigned to Alaskan peat.  
725 Top 10 contributing EFs were selected from both fresh and aged emissions. Since fresh and aged  
726 samples do not have the same set of compounds after the selection, we included the top 10  
727 compounds for both fresh and aged emissions. Hence, the number of top contributing compounds  
728 varies from one fuel to another. Solid bars of each type represent a chemical group from particulate  
729 emission of BB fuels and open bars of the same color represent gas phase BB emissions.

730

731 We have identified top contributing compounds for both fresh and aged BB emissions of each fuel  
732 to understand how emissions vary from one fuel to another. The top 10 compounds for fresh and  
733 aged emission were different, and we merged the top 10 compounds from fresh and aged emissions  
734 resulting in different numbers of total top compounds for different fuels. Here we discuss Alaskan  
735 peat emissions in their particulate phase (with solid bars) and gas phase (with open bars) as an  
736 example, while the remaining results are given in the SM. It is clear that the top compounds vary  
737 between fuels, likely because of the different chemical nature of these fuels.



738

739 Dehydroabietic acid, a resin acid, is the compound with the highest EF ( $92.2 \text{ mg kg}^{-1}$ ) for fresh  
740 combustion emissions from Alaskan peat. Moncarboxylic acids including palmitic acid ( $\text{EF} = 55.7$   
741  $\text{mg kg}^{-1}$ ), tetracosanoic acid ( $\text{EF} = 40.35 \text{ mg kg}^{-1}$ ), and docosanoic acid ( $\text{EF} = 35.38 \text{ mg kg}^{-1}$ ) were  
742 also found in high abundance in fresh emissions from the combustion of this fuel. The high  
743 contributions of  $\beta$ -sitosterol ( $\text{EF} = 36.84 \text{ mg kg}^{-1}$ ) and alkenoic acids (e.g., oleic acid  $\text{EF} = 52.1$   
744  $\text{mg kg}^{-1}$ ) to emissions are unique to Alaskan peat. All the compounds described above are found  
745 in particulate phase. After the OFR-oxidation, both dehydroabietic acid and  $\beta$ -sitosterol, considered  
746 to be potential markers for biomass burning emissions (Simoneit et al., 1993b), decreased from  
747  $91.9 \text{ mg kg}^{-1}$  to  $57.2 \text{ mg kg}^{-1}$  and  $36.8 \text{ mg kg}^{-1}$  to  $8.38 \text{ mg kg}^{-1}$  in particulate phase, respectively.  
748 This reduction in EF because of OFR oxidation for both dehydroabietic acid and  $\beta$ -sitosterol must  
749 be considered when using these compounds as biomass-burning markers. We observed the  
750 formation of low molecular weight organic compounds, particularly in gas phase, from OFR  
751 oxidation. For example, the EF of heptanoic acid increased from  $2.42 \text{ mg kg}^{-1}$  to  $16.9 \text{ mg kg}^{-1}$  and  
752 that of maleic acid increased from  $7.8 \text{ mg kg}^{-1}$  to  $107 \text{ mg kg}^{-1}$  in the gas phase because of OFR  
753 oxidation. Such a significant increase in the EF of maleic acid can be explained by the aqueous  
754 phase oxidation of methoxyphenols (El Zein et al., 2015) in the presence of ozone. We found that  
755 the oxidation inside the chamber was happening under dry conditions and understand that the  
756 reactions of organic compounds with OH radicals inside the OFR chamber will prevail over  
757 reactions with ozone. As we had our ozone scrubbers placed after sampling media (Fig. 1) to  
758 prevent the pumps and online instruments from ozone-induced damage, we suspect that the maleic  
759 acid was not formed inside the OFR chamber but rather by potential oxidation of organic  
760 compounds on filters with relatively longer exposure of ozone (40–60 min for smoldering  
761 combustion). Succinic acid EFs increased in both the gas phase (from  $0.0 \text{ mg kg}^{-1}$  to  $47.5 \text{ mg kg}^{-1}$ )  
762 and the particulate phase (from  $4.43 \text{ mg kg}^{-1}$  to  $33.5 \text{ mg kg}^{-1}$ ). Azelaic acid EFs showed mainly  
763 an increase in the particulate phase (from  $10.5 \text{ mg kg}^{-1}$  to  $33.1 \text{ mg kg}^{-1}$ ), and we think that this was  
764 because of the oxidation of oleic and eladic acid during OFR oxidation.

765

766

767

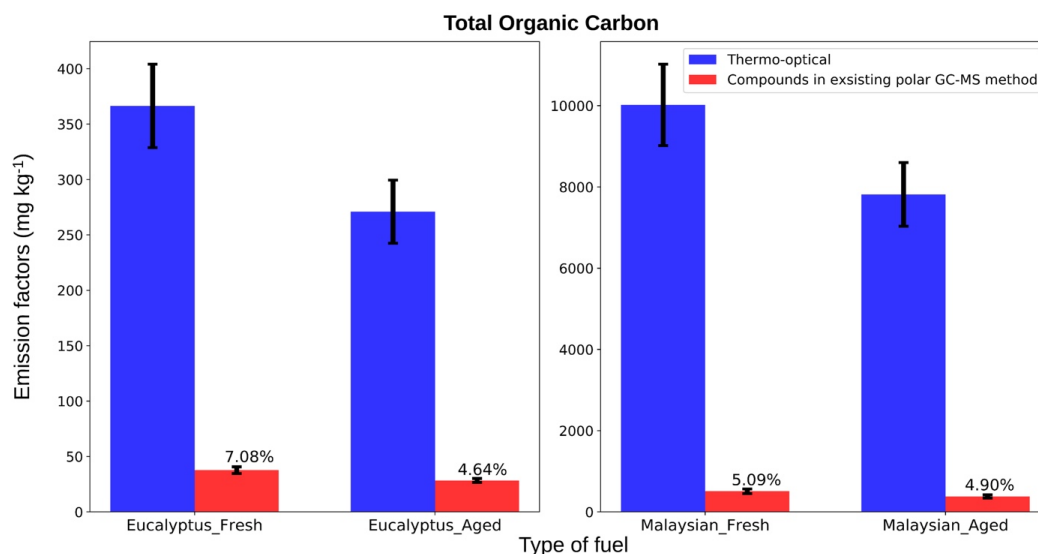
768

769



770  
771  
772  
773

### 3.5 Contribution of polar fraction to total organic carbon



774  
775  
776  
777  
778  
779  
780  
781

Figure 6. Contribution of GC-MS characterized polar compound carbon mass to total thermo-optical organic carbon mass. The y-axis shows the total carbon mass with dimensions of mass per mass. The error bars represent analytical uncertainties of the methods. For the thermo-optical method, uncertainties are the standard deviation of results from multiple punches on the same filter and for the GC-MS method, uncertainties were computed by taking the square root of sum of the squares of individual analytical uncertainties of all compounds included.

782 For Figure 6, we calculated the carbon content of total GC-MS characterized mass of identified  
783 polar organic compounds and compared results with the total OC mass characterized by the  
784 thermo-optical technique to estimate the contribution of polar compounds. The OC emissions were  
785 higher for smoldering combustion ( $10,209 \pm 5 \text{ mg kg}^{-1}$  for Malaysian peat fresh emissions) than  
786 for flaming combustion ( $366.5 \pm 7 \text{ mg kg}^{-1}$  for eucalyptus fresh emissions) samples, similar to the  
787 observation of flaming and smoldering combustion by Akagi et al. (2011). Total OC emissions  
788 are highly dependent on the type of fuel. For example, the fuel-based OC emission factor for rice  
789 crop residue burning is  $1960 \text{ mg kg}^{-1}$  (Cao et al., 2008), whereas burning of corn and conifer forest



790 yields emission factors of  $\sim 1457 \text{ mg kg}^{-1}$  (Andreae and Rosenfeld, 2008) and  $\sim 7800 \text{ mg kg}^{-1}$   
791 (Akagi et al., 2011a), respectively. Figure 6 shows that the 84 identified polar compounds in our  
792 study constituted 4.5% to 7% of total OC mass for both fresh and aged emissions. From Indonesian  
793 peat combustion emissions, Jayarathne et al. (2018) were able to identify polar compounds that  
794 constituted 5.446% of total organic carbon mass. In recent work, based on both a field campaign  
795 with prescribed burning and laboratory investigations, Jen et al. (2019) quantified a fraction (10–  
796 65%) of only identified compounds (not a fraction of total mass) by the use of the 2D-GC-MS  
797 technique. In our work, we identified only up to 7% (Fig. 6) of the total particle phase OC, and  
798 further analysis of unidentified compounds is needed to improve understanding of atmospheric  
799 chemistry of BB emissions.

800

801

### 802 3. Summary and conclusions

803 In this study, we chemically characterized the polar fraction of biomass-burning aerosols from  
804 laboratory combustion of six different globally and regionally important fuels—five of them  
805 representing smoldering and one of them representing flaming combustion. Our objective was to  
806 understand how emissions of the polar compounds (e.g., methoxyphenols) varied from one fuel to  
807 another during these combustion experiments and what are the relative distribution of these polar  
808 compounds in gas and particulate phase. We also identified the fates of these polar compounds  
809 following laboratory oxidation/aging (OFR aging). Resin acids were found mostly in emissions  
810 from combustion of peats from high latitude regions but not in emissions of tropical peatlands  
811 (e.g.,  $EF_{\text{group}} = 117 \pm 15 \text{ mg kg}^{-1}$  for Alaskan peat and  $EF_{\text{group}} = 4.0 \pm 0.5 \text{ mg kg}^{-1}$  for Malaysian peat).  
812 Similarly, monocarboxylic acids were found in higher abundance in emissions from high latitude  
813 peatlands compared to tropical peatland emissions (e.g.,  $EF_{\text{group}} = 505 \pm 36 \text{ mg kg}^{-1}$  for Alaskan peat  
814 and  $EF_{\text{group}} = 212 \pm 15 \text{ mg kg}^{-1}$  for Malaysian agricultural peat). The presence of both guaiacol and  
815 syringol moieties in all fuels indicated a part of the biomass, considered as representative of a  
816 particular geographical region, is deciduous for all fuels. Low molecular weight compounds are  
817 mostly found in gas phase (e.g., guaiacol found in gas phase 82–100%), whereas high molecular  
818 weight (e.g., high molecular weight monocarboxylic acids [ $>C_{16}$ ] more than 98% for all fuels) and  
819 highly oxygenated compounds (e.g., syringic acid and acetovanillone 65–100% in particulate



820 phase) are found in particulate phase with high abundance. Monocarboxylic acids (1.2–3 times)  
821 and methoxyphenols (1.5–2.5 times) decreased after OFR oxidation, whereas dicarboxylic acids  
822 increased by 3–9 times followed by OFR oxidation. Relatively low molecular weight hexanoic  
823 acid increased for both Malaysian (aged-to-fresh ratio =  $1.47 \pm 0.14$ ) and Malaysian agricultural  
824 peat (aged- to-fresh ratio =  $1.40 \pm 0.14$ ), whereas high molecular weight tetracosanoic acid ( $C_{20}$ )  
825 was reduced for all fuel increases (e.g., aged-to-fresh ratio =  $0.61 \pm 0.07$  for Malaysian peat). This  
826 indicated fragmentation occurring inside the OFR chamber. With relative distribution of the top  
827 10–15 compounds from Alaskan peat, we were able to identify transformation of unsaturated fatty  
828 acids (e.g., oleic acid) to dicarboxylic acids (e.g., azelaic acid). We identified only up to 7% of the  
829 total particle phase OC and further analysis of unidentified compounds with GC-MS full scan is  
830 needed for better understanding of atmospheric chemistry of BB emissions.

831

832

833 **Data availability.** Data can be provided upon request: <andrey.khlystov@dri.edu>.

834

835 **Author contributions.** DS, VS, and AK designed experiments. DS and CB performed sample and  
836 data collection. DS performed extractions, derivatizations, GC-MS analysis, summarized data, and  
837 wrote the paper. AW provided biomass fuels. VS, AK, and HM provided input on interpretation  
838 of results. VS, HM, and AK revised the manuscript.

839

840 **Competing interests.** The authors declare that they have no conflict of interest.

841

842 **Acknowledgements.** This research was supported by the National Science Foundation (NSF)  
843 under grant numbers AGS-1544425 and AGS-1408241, NASA ROSES under grant number  
844 NNX15AI48G, and internal funding from DRI. The authors would like to thank Anna Tsibar  
845 (Moscow State Lomonosov University, Moscow, Russia) for providing peat fuels from Russia.  
846 We acknowledge Benjamin Nault (CIRES, UC Boulder) and Andrew Lambe (Aerodyne) for their  
847 insightful discussion leading to identification of a potential artifact in our experimental set up  
848 associated with high maleic acid formation. The authors also thank Rodger Kreidberg for revising  
849 the manuscript.

850



851 REFERENCES

- 852 Akagi, S. K., Yokelson, R. J., Wiedinmyer, C., Alvarado, M. J., Reid, J. S., Karl, T., Crounse, J.  
853 D. and Wennberg, P. O.: Emission factors for open and domestic biomass burning for use in  
854 atmospheric models, *Atmos. Chem. Phys.*, 11(9), 4039–4072, doi:10.5194/acp-11-4039-2011,  
855 2011a.
- 856 Akagi, S. K., Yokelson, R. J., Wiedinmyer, C., Alvarado, M. J., Reid, J. S., Karl, T., Crounse, J.  
857 D. and Wennberg, P. O.: Emission factors for open and domestic biomass burning for use in  
858 atmospheric models, *Atmos. Chem. Phys.*, 11(9), 4039–4072, doi:10.5194/acp-11-4039-2011,  
859 2011b.
- 860 Alvarado, M. J., Lonsdale, C. R., Yokelson, R. J., Akagi, S. K., Coe, H., Craven, J. S., Fischer, E.  
861 V., McMeeking, G. R., Seinfeld, J. H., Soni, T., Taylor, J. W., Weise, D. R. and Wold, C. E.:  
862 Investigating the links between ozone and organic aerosol chemistry in a biomass burning plume  
863 from a prescribed fire in California chaparral, *Atmos. Chem. Phys.*, 15(12), 6667–6688,  
864 doi:10.5194/acp-15-6667-2015, 2015.
- 865 Andreae, M. O. and P. Merlet: Emission of trace gases and aerosols from biomass burning,  
866 *Global Biogeochem. Cycles*, 15(4), 955–966, doi:10.1029/2000GB001382, 2001.
- 867 Andreae, M. O. and Rosenfeld, D.: Aerosol-cloud-precipitation interactions. Part 1. The nature  
868 and sources of cloud-active aerosols, *Earth-Science Rev.*, 89(1–2), 13–41,  
869 doi:10.1016/j.earscirev.2008.03.001, 2008.
- 870 Arbex, M. A., Martins, L. C., Carvalho De Oliveira, R., Pereira, A. A., Arbex, F. F., Eduardo, J.,  
871 Cançado, D., Hilário, P., Saldiva, N., Luís, A. and Braga, F.: Air pollution from biomass burning  
872 and asthma hospital admissions in a sugar cane plantation area in Brazil, *J Epidemiol Community*  
873 *Heal.*, 61, 395–400, doi:10.1136/jech.2005.044743, 2007.
- 874 Asher, W. E., Pankow, J. F., Erdakos, G. B. and Seinfeld, J. H.: Estimating the vapor pressures of  
875 multi-functional oxygen-containing organic compounds using group contribution methods,  
876 *Atmos. Environ.*, 36(9), 1483–1498, doi:10.1016/S1352-2310(01)00564-7, 2002.
- 877 Bertrand, A., Stefenelli, G., Jen, C. N., Pieber, S. M., Bruns, E. A., Ni, H., Temime-Roussel, B.,  
878 Slowik, J. G., Goldstein, A. H., Haddad, I. El, Baltensperger, U., Prévôt, A. S. H., Wortham, H.  
879 and Marchand, N.: Evolution of the chemical fingerprint of biomass burning organic aerosol



- 880 during aging, *Atmos. Chem. Phys.*, 18(10), 7607–7624, doi:10.5194/acp-18-7607-2018, 2018.
- 881 Bhattarai, C., Samburova, V., Sengupta, D., Iaukea-lum, M. and Watt, A. C., Prichard, S.,  
882 Moosmüller, H. and Khlystov, A.: Physical and chemical characterization of aerosol in fresh and  
883 aged emissions from open combustion of biomass fuels, *Aerosol Sci. Technol.*, Accepted, 1–40,  
884 2018a.
- 885 Bhattarai, C., Samburova, V., Sengupta, D., Iaukea-lum, M., Watts, A. C., Moosmüller, H. and  
886 Khlystov, A.: Physical and chemical characterization of fresh and aged emissions from open  
887 combustion of biomass fuels, *Aerosol Sci. Technol.*, (Accepted),  
888 doi:10.1080/02786826.2018.1498585, 2018b.
- 889 Bhattarai, H., Saikawa, E., Wan, X., Zhu, H., Ram, K., Gao, S., Kang, S., Zhang, Q., Zhang, Y.,  
890 Wu, G., Wang, X., Kawamura, K., Fu, P. and Cong, Z.: Levoglucosan as a tracer of biomass  
891 burning: Recent progress and perspectives, *Atmos. Res.*, 220(September 2018), 20–33,  
892 doi:10.1016/j.atmosres.2019.01.004, 2019a.
- 893 Bhattarai, H., Saikawa, E., Wan, X., Zhu, H., Ram, K., Gao, S., Kang, S., Zhang, Q., Zhang, Y.,  
894 Wu, G., Wang, X., Kawamura, K., Fu, P. and Cong, Z.: Levoglucosan as a tracer of biomass  
895 burning: Recent progress and perspectives, *Atmos. Res.*, 220(September 2018), 20–33,  
896 doi:10.1016/j.atmosres.2019.01.004, 2019b.
- 897 Bonvalot, L., Tuna, T., Fagault, Y., Jaffrezo, J. L., Jacob, V., Chevrier, F. and Bard, E.: Estimating  
898 contributions from biomass burning, fossil fuel combustion, and biogenic carbon to carbonaceous  
899 aerosols in the Valley of Chamonix: A dual approach based on radiocarbon and levoglucosan,  
900 *Atmos. Chem. Phys.*, 16(21), 13753–13772, doi:10.5194/acp-16-13753-2016, 2016.
- 901 Cao, F., Zhang, S. C., Kawamura, K., Liu, X., Yang, C., Xu, Z., Fan, M., Zhang, W., Bao, M.,  
902 Chang, Y., Song, W., Liu, S., Lee, X., Li, J., Zhang, G. and Zhang, Y. L.: Chemical characteristics  
903 of dicarboxylic acids and related organic compounds in PM<sub>2.5</sub> during biomass-burning and non-  
904 biomass-burning seasons at a rural site of Northeast China, *Environ. Pollut.*, 231, 654–662,  
905 doi:10.1016/j.envpol.2017.08.045, 2017.
- 906 CAO, G., ZHANG, X., GONG, S. and ZHENG, F.: Investigation on emission factors of particulate  
907 matter and gaseous pollutants from crop residue burning, *J. Environ. Sci.*, 20(1), 50–55,  
908 doi:10.1016/S1001-0742(08)60007-8, 2008.





- 909 Carlton, A. G., Turpin, B. J., Altieri, K. E., Seitzinger, S., Reff, A., Lim, H. J. and Ervens, B.:  
910 Atmospheric oxalic acid and SOA production from glyoxal: Results of aqueous photooxidation  
911 experiments, *Atmos. Environ.*, 41(35), 7588–7602, doi:10.1016/j.atmosenv.2007.05.035, 2007.
- 912 Chakrabarty, R. K., Gyawali, M., Yatavelli, R. L. N., Pandey, A., Watts, A. C., Knue, J., Chen, L.  
913 W. A., Pattison, R. R., Tsibart, A., Samburova, V. and Moosmüller, H.: Brown carbon aerosols  
914 from burning of boreal peatlands: Microphysical properties, emission factors, and implications for  
915 direct radiative forcing, *Atmos. Chem. Phys.*, 16(5), 3033–3040, doi:10.5194/acp-16-3033-2016,  
916 2016.
- 917 Charbouillot, T., Gorini, S., Voyard, G., Parazols, M., Brigante, M., Deguillaume, L., Delort, A.  
918 M. and Mailhot, G.: Mechanism of carboxylic acid photooxidation in atmospheric aqueous phase:  
919 Formation, fate and reactivity, *Atmos. Environ.*, 56, 1–8, doi:10.1016/j.atmosenv.2012.03.079,  
920 2012.
- 921 Chow, J. C. and Watson, J. G.: Enhanced Ion Chromatographic Speciation of Water-Soluble PM  
922 2.5 to Improve Aerosol Source Apportionment, *Aerosol Sci. Eng.*, 1(1), 7–24,  
923 doi:10.1007/s41810-017-0002-4, 2017.
- 924 Chow, J. C., Watson, J. G., Pritchett, L. C., Pierson, W. R., Frazier, C. A. and Purcell, R. G.: The  
925 DRI thermal optical reflectance carbon analysis system - description, evaluation and applications  
926 in United-States air quality studies, *Atmos. Environ. Part a-General Top.*, 27(8), 1185–1201, 1993.
- 927 Chow, J. C., Watson, J. G., Chen, L. W. A., Arnott, W. P., Moosmüller, H. and Fung, K.:  
928 Equivalence of elemental carbon by thermal/optical reflectance and transmittance with different  
929 temperature protocols, *Environ. Sci. Technol.*, 38(16), 4414–4422, doi:10.1021/es034936u, 2004.
- 930 Decker, Z. C. J., Zarzana, K. J., Coggon, M., Min, K. E., Pollack, I., Ryerson, T. B., Peischl, J.,  
931 Edwards, P., Dubé, W. P., Markovic, M. Z., Roberts, J. M., Veres, P. R., Graus, M., Warneke, C.,  
932 De Gouw, J., Hatch, L. E., Barsanti, K. C. and Brown, S. S.: Nighttime Chemical Transformation  
933 in Biomass Burning Plumes: A Box Model Analysis Initialized with Aircraft Observations,  
934 *Environ. Sci. Technol.*, 53(5), 2529–2538, doi:10.1021/acs.est.8b05359, 2019.
- 935 Dills, R. L., Paulsen, M., Ahmad, J., Kalman, D. A., Elias, F. N. and Simpson, C. D.: Evaluation  
936 of urinary methoxyphenols as biomarkers of woodsmoke exposure, *Environ. Sci. Technol.*, 40(7),  
937 2163–2170, doi:10.1021/es051886f, 2006.



- 938 Ervens, B., Feingold, G., Frost, G. J. and Kreidenweis, S. M.: A modeling of study of aqueous  
939 production of dicarboxylic acids: 1. Chemical pathways and speciated organic mass production, *J.*  
940 *Geophys. Res. D Atmos.*, 109(15), 1–20, doi:10.1029/2003JD004387, 2004.
- 941 Fang, M., Zheng, M., Wang, F., To, K. L., Jaafar, A. B. and Tong, S. L.: The solvent-extractable  
942 organic compounds in the Indonesia biomass burning aerosols - Characterization studies, *Atmos.*  
943 *Environ.*, 33(5), 783–795, doi:10.1016/S1352-2310(98)00210-6, 1999.
- 944 Fine, P. M., Cass, G. R. and Simoneit, B. R. T.: Organic compounds in biomass smoke from  
945 residential wood combustion: Emissions characterization at a continental scale, *J. Geophys. Res.*  
946 *Atmos.*, 107(21), 1–9, doi:10.1029/2001JD000661, 2002.
- 947 Finlayson-Pitts, B. J. and Pitts Jr, J. N.: *Chemistry of the upper and lower atmosphere: theory,*  
948 *experiments, and applications*, Elsevier., 1999.
- 949 Fortenberry, C. F., Walker, M. J., Zhang, Y., Mitroo, D., Brune, W. H. and Williams, B. J.: Bulk  
950 and molecular-level characterization of laboratory-aged biomass burning organic aerosol from oak  
951 leaf and heartwood fuels, *Atmos. Chem. Phys.*, 18(3), 2199–2224, doi:10.5194/acp-18-2199-2018,  
952 2018.
- 953 Freimuth, E. J., Diefendorf, A. F., Lowell, T. V. and Wiles, G. C.: Sedimentary n-alkanes and n-  
954 alkanoic acids in a temperate bog are biased toward woody plants, *Org. Geochem.*, 128, 94–107,  
955 doi:10.1016/j.orggeochem.2019.01.006, 2019.
- 956 Goldstein, A. H. and Galbally, I. E.: Known and unexplored organic constituents in the earth's  
957 atmosphere, *Environ. Sci. Technol.*, 41(5), 1514–1521, doi:10.1021/es072476p, 2007.
- 958 Goodrick, S. L. and Stanturf, J. A.: Evaluating Potential Changes in Fire Risk from Eucalyptus  
959 Plantings in the Southern United States , *Int. J. For. Res.*, 2012, 1–9, doi:10.1155/2012/680246,  
960 2012.
- 961 Graham, B., Mayol-Bracero, O. L., Guyon, P., Roberts, G. C., Decesari, S., Facchini, M. C.,  
962 Artaxo, P., Maenhaut, W., Köll, P. and Andreae, M. O.: Water-soluble organic compounds in  
963 biomass burning aerosols over Amazonia 1. Characterization by NMR and GC-MS, *J. Geophys.*  
964 *Res. Atmos.*, 107(20), doi:10.1029/2001JD000336, 2002.
- 965 Grieshop, A. P., Donahue, N. M. and Robinson, A. L.: Laboratory investigation of photochemical  
966 oxidation of organic aerosol from wood fires 2: analysis of aerosol mass spectrometer data, *Atmos.*



- 967 Chem. Phys., 9, 2227–2240, doi:10.5194/acp-9-2227-2009, 2009.
- 968 Harden, J., Trumbore, S., Stocks, B., Hirsch, A., Gower, S., O’neill, K. and Kasischke, E.: The  
969 role of fire in the boreal carbon budget, *Glob. Chang. Biol.*, 6, 174–184, doi:10.1046/j.1365-  
970 2486.2000.06019.x, 2000.
- 971 Hawthorne, S. B., Krieger, M. S., Miller, D. J. and Mathiason, M. B.: Collection and Quantitation  
972 of Methoxylated Phenol Tracers for Atmospheric Pollution from Residential Wood Stoves,  
973 *Environ. Sci. Technol.*, 23(4), 470–475, doi:10.1021/es00181a013, 1989.
- 974 Hedges, J. I. and Ertel, J. R.: Characterization of Lignin by Gas Capillary Chromatography of  
975 Cupric Oxide Oxidation Products, *Anal. Chem.*, 54(2), 174–178, doi:10.1021/ac00239a007, 1982.
- 976 Hennigan, C. J., Sullivan, A. P., Collett, J. L. and Robinson, A. L.: Levoglucosan stability in  
977 biomass burning particles exposed to hydroxyl radicals, *Geophys. Res. Lett.*, 37(9), 2–5,  
978 doi:10.1029/2010GL043088, 2010.
- 979 Hills, W.E.; Brown, A. G. .: *Eucalypts for wood production.*, CSIRO., Canberra., 1978.
- 980 Hoffmann, D., Tilgner, A., Iinuma, Y. and Herrmann, H.: Atmospheric stability of levoglucosan:  
981 A detailed laboratory and modeling study, *Environ. Sci. Technol.*, 44(2), 694–699,  
982 doi:10.1021/es902476f, 2010.
- 983 Iinuma, Y., Brüggemann, E., Gnauk, T., Müller, K., Andreae, M. O., Helas, G., Parmar, R. and  
984 Herrmann, H.: Source characterization of biomass burning particles: The combustion of selected  
985 European conifers, African hardwood, savanna grass, and German and Indonesian peat, *J.*  
986 *Geophys. Res. Atmos.*, 112(8), doi:10.1029/2006JD007120, 2007.
- 987 Jayarathne, T., Stockwell, C. E., Gilbert, A. A., Daugherty, K., Cochrane, M. A., Ryan, K. C.,  
988 Putra, E. I., Saharjo, B. H., Nurhayati, A. D., Albar, I., Yokelson, R. J. and Stone, E. A.: Chemical  
989 characterization of fine particulate matter emitted by peat fires in Central Kalimantan, Indonesia,  
990 during the 2015 El Niño, *Atmos. Chem. Phys.*, 18(4), 2585–2600, doi:10.5194/acp-18-2585-2018,  
991 2018.
- 992 Jen, C. N., Hatch, L. E., Selimovic, V., Yokelson, R. J., Weber, R., Fernandez, A. E., Kreisberg,  
993 N. M., Barsanti, K. C. and Goldstein, A. H.: Speciated and total emission factors of particulate  
994 organics from burning western US wildland fuels and their dependence on combustion efficiency,  
995 *Atmos. Chem. Phys.*, 19(2), 1013–1026, doi:10.5194/acp-19-1013-2019, 2019.



- 996 Jimenez, J. L., Canagaratna, M. R., Donahue, N. M., Prevot, A. S. H., Zhang, Q., Kroll, J. H.,  
997 DeCarlo, P. F., Allan, J. D., Coe, H., Ng, N. L., Aiken, A. C., Docherty, K. S., Ulbrich, I. M.,  
998 Grieshop, A. P., Robinson, A. L., Duplissy, J., Smith, J. D., Wilson, K. R., Lanz, V. A., Hueglin,  
999 C., Sun, Y. L., Tian, J., Laaksonen, A., Raatikainen, T., Rautiainen, J., Vaattovaara, P., Ehn, M.,  
1000 Kulmala, M., Tomlinson, J. M., Collins, D. R., Cubison, M. J., Dunlea, E. J., Huffman, J. A.,  
1001 Onasch, T. B., Alfarra, M. R., Williams, P. I., Bower, K., Kondo, Y., Schneider, J., Drewnick, F.,  
1002 Borrmann, S., Weimer, S., Demerjian, K., Salcedo, D., Cottrell, L., Griffin, R., Takami, A.,  
1003 Miyoshi, T., Hatakeyama, S., Shimono, A., Sun, J. Y., Zhang, Y. M., Dzepina, K., Kimmel, J. R.,  
1004 Sueper, D., Jayne, J. T., Herndon, S. C., Trimborn, A. M., Williams, L. R., Wood, E. C.,  
1005 Middlebrook, A. M., Kolb, C. E., Baltensperger, U. and Worsnop, D. R.: Evolution of organic  
1006 aerosols in the atmosphere, *Science* (80-. ), 326(5959), 1525–1529, doi:10.1126/science.1180353,  
1007 2009.
- 1008 Jung, J., Lyu, Y., Lee, M., Hwang, T., Lee, S. and Oh, S.: Impact of Siberian forest fires on the  
1009 atmosphere over the Korean Peninsula during summer 2014, *Atmos. Chem. Phys.*, 16(11), 6757–  
1010 6770, doi:10.5194/acp-16-6757-2016, 2016.
- 1011 Karlberg, A.-T., Boman, A., Hacksell, U., Jacobsson, S. and Nilsson, J. L. G.: Contact allergy to  
1012 dehydroabiestic acid derivatives isolated from Portuguese colophony, *Contact Dermatitis*, 19(3),  
1013 166–174, 1988.
- 1014 Kawamura, K. and Bikkina, S.: A review of dicarboxylic acids and related compounds in  
1015 atmospheric aerosols: Molecular distributions, sources and transformation, *Atmos. Res.*, 170, 140–  
1016 160, doi:10.1016/j.atmosres.2015.11.018, 2016.
- 1017 Kessler, S. H., Smith, J. D., Che, D. L., Worsnop, D. R., Wilson, K. R. and Kroll, J. H.: Chemical  
1018 Sinks of Organic Aerosol: Kinetics and Products of the Heterogeneous Oxidation of Erythritol and  
1019 Levoglucosan, *Environ. Sci. Technol.*, 44(18), 7005–7010, doi:10.1021/es101465m, 2010.
- 1020 Kundu, S., Kawamura, K., Andreae, T. W., Hoffer, A. and Andreae, M. O.: Molecular distributions  
1021 of dicarboxylic acids, ketocarboxylic acids and  $\alpha$ -dicarbonyls in biomass burning aerosols:  
1022 implications for photochemical production and degradation in smoke layers, *Atmos. Chem. Phys.*,  
1023 10(5), 2209–2225, doi:10.5194/acp-10-2209-2010, 2010.
- 1024 Legrand, M., McConnell, J., Fischer, H., Wolff, E. W., Preunkert, S., Chellman, N., Leuenberger,



- 1025 D., Maselli, O., Sigl, M., Schüpbach, S. and Flannigan, M.: Boreal fire records in Northern  
1026 Hemisphere ice cores: A review, *Clim. Past Discuss.*, (July), 1–43, doi:10.5194/cp-2016-70, 2016.
- 1027 Li, R., Palm, B. B., Ortega, A. M., Hlywiak, J., Hu, W., Peng, Z., Day, D. A., Knote, C., Brune,  
1028 W. H., de Gouw, J. A. and Jimenez, J. L.: Modeling the Radical Chemistry in an Oxidation Flow  
1029 Reactor: Radical Formation and Recycling, Sensitivities, and the OH Exposure Estimation  
1030 Equation., *J. Phys. Chem. A*, 119(19), 4418–4432, doi:10.1021/jp509534k, 2015.
- 1031 Liu, X., Huey, L. G., Yokelson, R. J., Selimovic, V., Simpson, I. J., Müller, M., Jimenez, J. L.,  
1032 Campuzano-Jost, P., Beyersdorf, A. J., Blake, D. R., Butterfield, Z., Choi, Y., Crounse, J. D., Day,  
1033 D. A., Diskin, G. S., Dubey, M. K., Fortner, E., Hanisco, T. F., Hu, W., King, L. E., Kleinman, L.,  
1034 Meinardi, S., Mikoviny, T., Onasch, T. B., Palm, B. B., Peischl, J., Pollack, I. B., Ryerson, T. B.,  
1035 Sachse, G. W., Sedlacek, A. J., Shilling, J. E., Springston, S., St. Clair, J. M., Tanner, D. J., Teng,  
1036 A. P., Wennberg, P. O., Wisthaler, A. and Wolfe, G. M.: Airborne measurements of western U.S.  
1037 wildfire emissions: Comparison with prescribed burning and air quality implications, *J. Geophys.*  
1038 *Res.*, 122(11), 6108–6129, doi:10.1002/2016JD026315, 2017.
- 1039 Maenhaut, W., Vermeylen, R., Claeys, M., Vercauteren, J. and Roekens, E.: Sources of the PM10  
1040 aerosol in Flanders, Belgium, and re-assessment of the contribution from wood burning, *Sci. Total*  
1041 *Environ.*, 562, 550–560, doi:10.1016/j.scitotenv.2016.04.074, 2016.
- 1042 Mazzoleni, L. R., Zielinska, B. and Moosmüller, H.: Emissions of levoglucosan, methoxy phenols,  
1043 and organic acids from prescribed burns, laboratory combustion of wildland fuels, and residential  
1044 wood combustion, *Environ. Sci. Technol.*, 41(7), 2115–2122, doi:10.1021/es061702c, 2007.
- 1045 Müller-Tautges, C., Eichler, A., Schwikowski, M., Pezzatti, G. B., Conedera, M. and Hoffmann,  
1046 T.: Historic records of organic compounds from a high Alpine glacier: Influences of biomass  
1047 burning, anthropogenic emissions, and dust transport, *Atmos. Chem. Phys.*, 16(2), 1029–1043,  
1048 doi:10.5194/acp-16-1029-2016, 2016.
- 1049 Net, S., Alvarez, E. G., Gligorovski, S. and Wortham, H.: Heterogeneous reactions of ozone with  
1050 methoxyphenols, in presence and absence of light, *Atmos. Environ.*, 45(18), 3007–3014,  
1051 doi:10.1016/j.atmosenv.2011.03.026, 2011.
- 1052 Oros, D. R. and Simoneit, B. R. T.: Identification and emission factors of molecular tracers in  
1053 organic aerosols from biomass burning Part 1. Temperate climate conifers., 2001a.



- 1054 Oros, D. R. and Simoneit, B. R. T.: Identification and emission factors of molecular tracers in  
1055 organic aerosols from biomass burning Part 2. Deciduous trees, *Appl. Geochemistry*, 16(13),  
1056 1545–1565, doi:[https://doi.org/10.1016/S0883-2927\(01\)00022-1](https://doi.org/10.1016/S0883-2927(01)00022-1), 2001b.
- 1057 Oros, D. R., Abas, M. R. bin, Omar, N. Y. M. J., Rahman, N. A. and Simoneit, B. R. T.:  
1058 Identification and emission factors of molecular tracers in organic aerosols from biomass burning:  
1059 Part 3. Grasses, *Appl. Geochemistry*, 21(6), 919–940, doi:10.1016/j.apgeochem.2006.01.008,  
1060 2006.
- 1061 Ortega, A. M., Day, D. A., Cubison, M. J., Brune, W. H., Bon, D., de Gouw, J. A. and Jimenez, J.  
1062 L.: Secondary organic aerosol formation and primary organic aerosol oxidation from biomass-  
1063 burning smoke in a flow reactor during FLAME-3, *Atmos. Chem. Phys.*, 13(22), 11551–11571,  
1064 doi:10.5194/acp-13-11551-2013, 2013.
- 1065 Pankow, J. F. and Asher, W. E.: SIMPOL.1: A simple group contribution method for predicting  
1066 vapor pressures and enthalpies of vaporization of multifunctional organic compounds, *Atmos.*  
1067 *Chem. Phys.*, 8(10), 2773–2796, doi:10.5194/acp-8-2773-2008, 2008.
- 1068 Park, R. J., Jacob, D. J. and Logan, J. A.: Fire and biofuel contributions to annual mean aerosol  
1069 mass concentrations in the United States, *Atmos. Environ.*, 41(35), 7389–7400,  
1070 doi:10.1016/j.atmosenv.2007.05.061, 2007.
- 1071 Penner, J. E., Ghan, S. J. and Walton, J. J.: The role of biomass burning in the budget and cycle of  
1072 carbonaceous soot aerosols and their climate impact, [online] Available from:  
1073 [https://inis.iaea.org/search/search.aspx?orig\\_q=RN:23067068](https://inis.iaea.org/search/search.aspx?orig_q=RN:23067068) (Accessed 8 September 2019),  
1074 1991.
- 1075 Ramanathan, V. and Carmichael, G.: Global and regional climate changes due to black carbon,  
1076 *Nat. Geosci.*, 1(4), 221–227, doi:10.1038/ngeo156, 2008.
- 1077 Regalado, J., Pérez-Padilla, R., Sansores, R., Ramirez, J. I. P., Brauer, M., Paré, P. and Vedal, S.:  
1078 The effect of biomass burning on respiratory symptoms and lung function in rural Mexican  
1079 women, *Am. J. Respir. Crit. Care Med.*, 174(8), 901–905, doi:10.1164/rccm.200503-479OC,  
1080 2006.
- 1081 Rinehart, L. R., Fujita, E. M., Chow, J. C., Magliano, K. and Zielinska, B.: Spatial distribution of  
1082 PM<sub>2.5</sub> associated organic compounds in central California, *Atmos. Environ.*, 40(2), 290–303,



- 1083 doi:10.1016/j.atmosenv.2005.09.035, 2006.
- 1084 Sadhra, S., Foulds, I. S. and Gray, C. N.: Oxidation of resin acids in colophony (rosin) and its  
1085 implications for patch testing, *Contact Dermatitis*, 39(2), 58–63, doi:10.1111/j.1600-  
1086 0536.1998.tb05833.x, 1998.
- 1087 Samburova, V., Hallar, A. G., Mazzoleni, L. R., Saranjampour, P., Lowenthal, D., Kohl, S. D. and  
1088 Zielinska, B.: Composition of water-soluble organic carbon in non-urban atmospheric aerosol  
1089 collected at the Storm Peak Laboratory, *Environ. Chem.*, 10(5), 370–380 [online] Available from:  
1090 <https://doi.org/10.1071/EN13079>, 2013.
- 1091 Samburova, V., Connolly, J., Gyawali, M., Yatavelli, R. L. N., Watts, A. C., Chakrabarty, R. K.,  
1092 Zielinska, B., Moosmüller, H. and Khlystov, A.: Polycyclic aromatic hydrocarbons in biomass-  
1093 burning emissions and their contribution to light absorption and aerosol toxicity, *Sci. Total*  
1094 *Environ.*, 568, 391–401, doi:10.1016/j.scitotenv.2016.06.026, 2016.
- 1095 Sarkanen, K. V and Ludwig, C. H.: *Lignins: occurrence, formation, structure and reactions*, Wiley-  
1096 interscience, New York., 1971.
- 1097 Schauer, J. J., Kleeman, M. J., Cass, G. R. and Simoneit, B. R. T.: Measurement of emissions from  
1098 air pollution sources. 3. C1-C29 organic compounds from fireplace combustion of wood, *Environ.*  
1099 *Sci. Technol.*, 35(9), 1716–1728, doi:10.1021/es001331e, 2001a.
- 1100 Schauer, J. J., Kleeman, M. J., Cass, G. R. and Simoneit, B. R. T.: Measurement of emissions from  
1101 air pollution sources. 3. C1-C29 organic compounds from fireplace combustion of wood, *Environ.*  
1102 *Sci. Technol.*, 35(9), 1716–1728, doi:10.1021/es001331e, 2001b.
- 1103 Schmidl, C., Marr, I. L., Caseiro, A., Kotianová, P., Berner, A., Bauer, H., Kasper-Giebl, A. and  
1104 Puxbaum, H.: Chemical characterisation of fine particle emissions from wood stove combustion  
1105 of common woods growing in mid-European Alpine regions, *Atmos. Environ.*, 42(1), 126–141,  
1106 doi:10.1016/j.atmosenv.2007.09.028, 2008a.
- 1107 Schmidl, C., Bauer, H., Dattler, A., Hitzenberger, R., Weissenboeck, G., Marr, I. L. and Puxbaum,  
1108 H.: Chemical characterisation of particle emissions from burning leaves, *Atmos. Environ.*, 42(40),  
1109 9070–9079, doi:10.1016/j.atmosenv.2008.09.010, 2008b.
- 1110 Schnitzler, E. G. and Abbatt, J. P. D.: Heterogeneous OH oxidation of secondary brown carbon  
1111 aerosol, *Atmos. Chem. Phys.*, 18(19), 14539–14553, doi:10.5194/acp-18-14539-2018, 2018.



- 1112 Sengupta, D., Samburova, V., Bhattarai, C., Kirillova, E., Mazzoleni, L., Iaukea-Lum, M., Watts,  
1113 A., Moosmüller, H. and Khlystov, A.: Light absorption by polar and non-polar aerosol compounds  
1114 from laboratory biomass combustion, *Atmos. Chem. Phys. Discuss.*, (March), 1–45,  
1115 doi:10.5194/acp-2018-161, 2018.
- 1116 Simoneit, B. R. T.: Biomass burning — a review of organic tracers for smoke from incomplete  
1117 combustion, *Appl. Geochemistry*, 17(3), 129–162, doi:https://doi.org/10.1016/S0883-  
1118 2927(01)00061-0, 2002.
- 1119 Simoneit, B. R. T., Schauer, J. J., Nolte, C. G., Oros, D. R., Elias, V. O., Fraser, M. P., Rogge, W.  
1120 F. and Cass, G. R.: Levoglucosan, a tracer for cellulose in biomass burning and atmospheric  
1121 particles, *Atmos. Environ.*, 33(2), 173–182, doi:10.1016/S1352-2310(98)00145-9, 1999.
- 1122 Simonelt, B. R. T., Rogge, W. F., Mazurek, M. A., Standley, L. J., Hildemann, L. M. and Cass, G.  
1123 R.: Lignin Pyrolysis Products, Lignans, and Resin Acids as Specific Tracers of Plant Classes in  
1124 Emissions from Biomass Combustion, *Environ. Sci. Technol.*, 27(12), 2533–2541,  
1125 doi:10.1021/es00048a034, 1993a.
- 1126 Simonelt, B. R. T., Rogge, W. F., Mazurek, M. A., Standley, L. J., Hildemann, L. M. and Cass, G.  
1127 R.: Lignin Pyrolysis Products, Lignans, and Resin Acids as Specific Tracers of Plant Classes in  
1128 Emissions from Biomass Combustion, *Environ. Sci. Technol.*, 27(12), 2533–2541,  
1129 doi:10.1021/es00048a034, 1993b.
- 1130 Simpson, C. D. and Naeher, L. P.: Biological monitoring of wood-smoke exposure, *Inhal. Toxicol.*,  
1131 22(2), 99–103, doi:10.3109/08958370903008862, 2010.
- 1132 Tan, Y., Lim, Y. B., Altieri, K. E., Seitzinger, S. P. and Turpin, B. J.: Mechanisms leading to  
1133 oligomers and SOA through aqueous photooxidation: Insights from OH radical oxidation of acetic  
1134 acid and methylglyoxal, *Atmos. Chem. Phys.*, 12(2), 801–813, doi:10.5194/acp-12-801-2012,  
1135 2012.
- 1136 Tian, J., Chow, J. C., Cao, J., Han, Y., Ni, H., Chen, L. A., Wang, X., Huang, R., Moosmüller, H.  
1137 and Watson, J. G.: A Biomass Combustion Chamber : Design , Evaluation , and a Case Study of  
1138 Wheat Straw Combustion Emission Tests , 2104–2114, doi:10.4209/aaqr.2015.03.0167, 2015.
- 1139 Turetsky, M. R., Benscoter, B., Page, S., Rein, G., Van Der Werf, G. R. and Watts, A.: Global  
1140 vulnerability of peatlands to fire and carbon loss, *Nat. Geosci.*, 8(1), 11–14,





- 1141 doi:10.1038/ngeo2325, 2015.
- 1142 Wan, X., Kawamura, K., Ram, K., Kang, S., Loewen, M., Gao, S., Wu, G., Fu, P., Zhang, Y.,  
1143 Bhattarai, H. and Cong, Z.: Aromatic acids as biomass-burning tracers in atmospheric aerosols and  
1144 ice cores: A review, *Environ. Pollut.*, 247, 216–228, doi:10.1016/j.envpol.2019.01.028, 2019.
- 1145 Yang, X. Y., Igarashi, K., Tang, N., Lin, J. M., Wang, W., Kameda, T., Toriba, A. and Hayakawa,  
1146 K.: Indirect- and direct-acting mutagenicity of diesel, coal and wood burning-derived particulates  
1147 and contribution of polycyclic aromatic hydrocarbons and nitropolycyclic aromatic hydrocarbons,  
1148 *Mutat. Res. - Genet. Toxicol. Environ. Mutagen.*, 695(1–2), 29–34,  
1149 doi:10.1016/j.mrgentox.2009.10.010, 2010.
- 1150 Yatavelli, R. L. N., Chen, L.-W. A., Knue, J., Samburova, V., Gyawali, M., Watts, A. C.,  
1151 Chakrabarty, R. K., Moosmüller, H., Hodzic, A., Wang, X., Zielinska, B., Chow, J. C. and Watson,  
1152 J. G.: Emissions and Partitioning of Intermediate-Volatility and Semi-Volatile Polar Organic  
1153 Compounds (I/SV-POCs) During Laboratory Combustion of Boreal and Sub-Tropical Peat,  
1154 *Aerosol Sci. Eng.*, 1(1), 25–32, doi:10.1007/s41810-017-0001-5, 2017a.
- 1155 Yatavelli, R. L. N., Chen, L.-W. A., Knue, J., Samburova, V., Gyawali, M., Watts, A. C.,  
1156 Chakrabarty, R. K., Moosmüller, H., Hodzic, A., Wang, X., Zielinska, B., Chow, J. C. and Watson,  
1157 J. G.: Emissions and Partitioning of Intermediate-Volatility and Semi-Volatile Polar Organic  
1158 Compounds (I/SV-POCs) During Laboratory Combustion of Boreal and Sub-Tropical Peat,  
1159 *Aerosol Sci. Eng.*, 1(1), 25–32, doi:10.1007/s41810-017-0001-5, 2017b.
- 1160 Yee, L. D., Kautzman, K. E., Loza, C. L., Schilling, K. A., Coggon, M. M., Chhabra, P. S., Chan,  
1161 M. N., Chan, A. W. H., Hersey, S. P., Crouse, J. D., Wennberg, P. O., Flagan, R. C. and Seinfeld,  
1162 J. H.: Secondary organic aerosol formation from biomass burning intermediates: Phenol and  
1163 methoxyphenols, *Atmos. Chem. Phys.*, 13(16), 8019–8043, doi:10.5194/acp-13-8019-2013, 2013.
- 1164 Yokelson, R. J., Bertschi, I. T., Christian, T. J., Hobbs, P. V., Ward, D. E. and Hao, W. M.: Trace  
1165 gas measurements in nascent, aged, and cloud-processed smoke from African savanna fires by  
1166 airborne Fourier transform infrared spectroscopy (AFTIR), *J. Geophys. Res. Atmos.*, 108(D13),  
1167 n/a-n/a, doi:10.1029/2002JD002322, 2003.
- 1168 El Zein, A., Coeur, C., Obeid, E., Lauraguais, A. and Fagniez, T.: Reaction Kinetics of Catechol  
1169 (1,2-Benzenediol) and Guaiacol (2-Methoxyphenol) with Ozone, *J. Phys. Chem. A*, 119(26),



- 1170 6759–6765, doi:10.1021/acs.jpca.5b00174, 2015.
- 1171 Zhu, Y., Yang, L., Chen, J., Kawamura, K., Sato, M., Tilgner, A., van Pinxteren, D., Chen, Y.,  
1172 Xue, L., Wang, X., Herrmann, H. and Wang, W.: Molecular distributions of dicarboxylic acids,  
1173 oxocarboxylic acids, and  $\alpha$ -dicarbonyls in  
1174 PM<sub>2.5</sub> collected at Mt. Tai, in North China in 2014, Atmos. Chem. Phys.  
1175 Discuss., 1–31, doi:10.5194/acp-2017-1240, 2018.
- 1176
- 1177
- 1178